CHALMERS
UNIVERSITY OF TECHNOLOGY

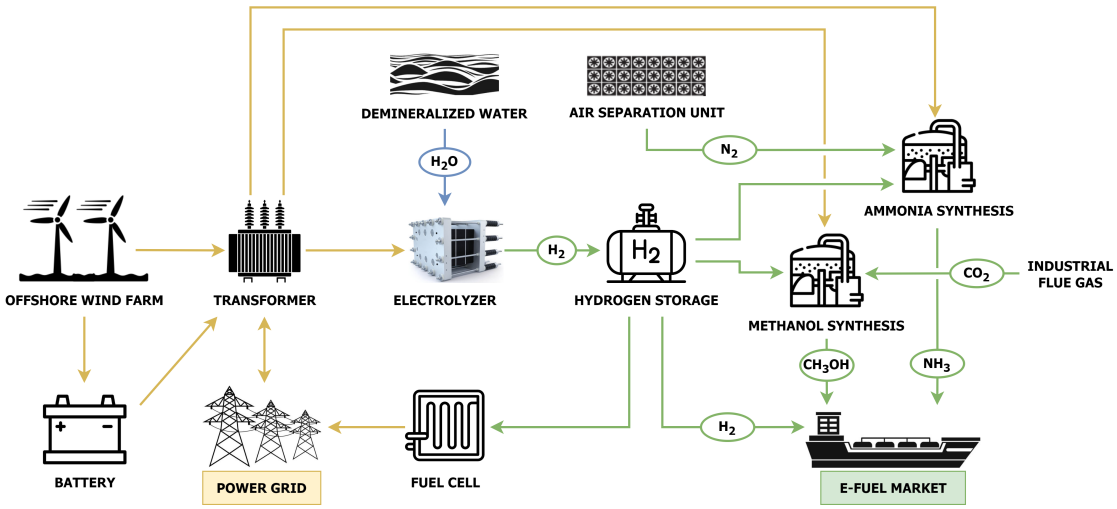

Techno-economical evaluation of an e-fuel-producing wind farm system focusing on hydrogen, ammonia and methanol production

Master's thesis in Sustainable Energy Systems

CARL JÖNSSON LINDHOLM

Department of Mechanics and Maritime Science

CHALMERS UNIVERSITY OF TECHNOLOGY
Gothenburg, Sweden 2023
www.chalmers.se

Master's thesis 2023

Techno-economical evaluation of an e-fuel-producing wind farm system focusing on hydrogen, ammonia and methanol production

CARL JÖNSSON LINDHOLM

Department of Mechanics and Maritime Science
Division of Maritime Studies
Unit of Maritime Environmental Sciences
Chalmers University of Technology
Gothenburg, Sweden 2023

Techno-economical evaluation of an e-fuel-producing wind farm system focusing on hydrogen, ammonia and methanol production
CARL JÖNSSON LINDHOLM

© CARL JÖNSSON LINDHOLM, 2023.

Academic supervisor: Maria Grahn, Department of Mechanics and Maritime Science
Supervisor: Robert Sandén, Euromekanik AB
Examiner: Selma Brynolf, Department of Mechanics and Maritime Science

Master's Thesis 2023
Department of Mechanics and Maritime Science
Division of Maritime Studies
Unit of Maritime Environmental Sciences
Chalmers University of Technology
SE-412 96 Gothenburg
Telephone +46 31 772 1000

Cover: Infrastructure of the modelled energy system, consisting of a wind farm, battery, fuel cell, electrolyzer, hydrogen storage and various production facilities connected to the methanol and ammonia synthesis.

Typeset in LaTeX
Printed by Chalmers Reproservice
Gothenburg, Sweden 2023

Techno-economical evaluation of an e-fuel-producing wind farm system focusing on hydrogen, ammonia and methanol production

CARL JÖNSSON LINDHOLM
Department of Mechanics and Maritime Science
Division of Maritime Studies
Chalmers University of Technology

Abstract

Given that the share of renewable energy sources will increase in future energy systems, coupling e-fuel production plants with intermittent electricity will be beneficial. This study evaluates the techno-economical feasibility of hydrogen, ammonia and methanol production using electricity produced from a connected wind farm. A model was developed to also include grid interactions and the possibility to utilize batteries and fuel cells. Different cases and scenarios were assumed, and technical behaviours along with the profitability of investments were evaluated. Furthermore, an understanding of the power-to-x concept and its associated investment strategies was developed to display trends and behaviours in the system. The results of this study are however limited to some extent. Technical dynamics such as ramping times and hot standby of for example the ammonia and methanol production, were restrained by an hourly resolution together with software limitations.

It was seen that peak-load shifting using batteries could increase profits and that a battery investment was beneficial seen to the additional amount of electricity supplied to the grid. Using fuel cells and electrolyzers did not increase profits but could still pose a viable option in a scenario where the utilized wind energy has to be maximized. Regardless, batteries were seen to decrease profits when utilized to support hydrogen production, in spite of the fact that hydrogen production was increased. Electricity prices and grid transfer capacities were seen to have a significant impact on the system which led to them being key parameters utilized to nuance the results. System configurations that maximized the profit could be found for the different cases, and results point toward ammonia likely being the most profitable option, even if methanol offers a more flexible synthesis with the hot-standby option. The main takeaway, however, is that the profitability of an e-fuel-producing energy system is significantly affected by the e-fuel market prices. For example, ammonia production was seen to give the highest profits, in the scenario with a market price of 1,000-1,500 €/ton$_{NH_3}$, at around 3,000 M€ over the 20-year lifetime. Hydrogen could also compete with ammonia at a price of 5.5 €/kg$_{H_2}$, and had a higher profitability when the ammonia price went below 1,500 €/ton$_{NH_3}$ at 1,500 M€.

Keywords: power-to-x, electrolysis, electrofuels, power-to-fuels, PTX, synthetic fuels, energy storage system, cost, profit

Acknowledgements

I would like to devote my sincerest gratitude to my supervisors Maria Grahn and Robert Sandén, for their encouragement and guidance during this thesis work. My supervisors, along with my colleagues at Euromekanik (Peter, Cecilia, Pär and Amanda), have supported me throughout this process and for that I am deeply grateful. They have helped me to overcome difficulties both in the thesis writing and methodology of the study, and they truly enabled me to reach my full potential. I would also like to thank Benjamin Guinot at Seed Energy, for his quick responses concerning any issue I experienced with the software. Benjamin coordinated several meetings to discuss the different functions of the software. Anytime I had trouble interpreting results or debugging my model, his support was crucial and educative, allowing me to broaden the study's perspective. Benjamin even reconstructed an entire control algorithm (Algorithm 5, Table 3.1) for it to serve a certain purpose in this study.

Carl Jönsson Lindholm, Gothenburg, June 2023

List of Acronyms, Terminology, Cases and Key parameters

Acronyms

BoL	Beginning of lifetime
CCS	Carbon capture and storage
CO_2	Carbon dioxide
DEA	Danish Energy Agency
DLR	Dynamic line rating
DoD	Depth of discharge
DTR	Dynamic transformer rating
EoL	End of lifetime
H_2	Hydrogen
HB	Haber-Bosch
IEA	International Energy Agency
MeOH	Methanol
NH_3	Ammonia
O_2	Oxygen
O&M	Operations and maintenance
PBT	Payback time
RES	Renewable-based energy sources
SEA	Swedish Energy Agency
SLR	Static line rating
SoC	State of charge
STR	Static transformer rating
TSO	Transmission system operator
VMS	Variational management strategy
UWE	Utilized wind energy

SE4 2019	Electricity prices in the SE4 bidding area (Sweden) in 2019
SE4 2022	Electricity prices in the SE4 bidding area (Sweden) in 2022

Terminology

Case	A main setup of the system, depending on production objective.
Con guration	Speci c setup of a case or scenario, e.g. speci ed transfer capacity and electricity price.
E-fuel	A synthetic fuel produced from electrolysis of water, and in certain cases CO_2/N_2 (e.g. ammonia and methanol).
Peak-load shifting	A VMS used to transfer electricity demands to a di erent time interval, with for example batteries or fuel cells and electrolyzers.
Pro t	Software output, the di erence between the total incomes and expenses over the system lifetime.
Scenario	Sub-case with di erent technologies applied, e.g. peak-shifting with batteries.

Cases

Ammonia case	The system's main objective is ammonia production.
Grid support case	The system's main objective is supporting the grid with electricity injections.
Hydrogen case	The system's main objective is hydrogen production.
Methanol case	The system's main objective is methanol production.

Key parameters

1 GW_{peak}	Transformer limited by a varying transfer capacity with a maximum of 1 GW.
500 $MW_{constant}$	Transformer limited by a constant transfer capacity of 500 MW.
500 MW_{peak}	Transformer limited by a varying transfer capacity with a maximum of 500 MW.

Contents

List of Acronyms ix

List of Figures xvii

List of Tables xxiii

1 Introduction 1
1.1 Aim . . . 3
1.2 Methodology . . . 3

2 Theoretical background 5
2.1 Variational Management Strategy . . . 5
2.2 O shore large-scale wind farm . . . 6
2.2.1 Wind farm characteristics . . . 6
2.3 Power grid . . . 8
2.3.1 Power grid characteristics . . . 8
2.4 Batteries . . . 10
2.4.1 Battery characteristics . . . 11
2.5 Proton exchange membrane . . . 12
2.5.1 Electrolyzer characteristics . . . 15
2.5.2 Fuel cell characteristics . . . 17
2.6 Hydrogen storage . . . 18
2.6.1 Storage characteristics . . . 19
2.7 Ammonia synthesis . . . 21
2.7.1 Synthesis characteristics . . . 21
2.8 Methanol synthesis and carbon capture . . . 23
2.8.1 Synthesis characteristics . . . 24
2.9 Energy system economics . . . 26

3 Method 27
3.1 The system under study . . . 27
3.2 Study framework . . . 27
3.3 Model framework . . . 28
3.3.1 Controllers . . . 29
3.3.2 Cases . . . 31

4 Results 33

4.1 Electrolyzer standby . . . 33
4.2 Grid support case . . . 34
4.2.1 Electricity price . . . 34
4.2.2 Transfer capacity . . . 35
4.2.3 Peak-load shifting scenario . . . 36
4.2.3.1 Batteries . . . 36
4.2.3.2 Hydrogen . . . 37
4.2.3.3 Investment strategy . . . 39
4.3 Hydrogen case . . . 40
4.3.1 Batteries . . . 43
4.4 Ammonia and methanol case . . . 44
4.4.1 Operational dynamics . . . 45
4.4.2 Optimization process . . . 46
4.4.2.1 Ammonia production . . . 46
4.4.2.2 Methanol production . . . 48
4.4.3 Economic performance . . . 51
4.4.3.1 500 MW transfer capacity . . . 52
4.4.4 Battery addition . . . 54
4.5 Investment recommendations . . . 54

5 Discussion 57
5.1 Technical uncertainties . . . 57
5.1.1 Heat integration . . . 57
5.1.2 System developments . . . 58
5.1.3 Scaling the system . . . 58
5.1.4 Investment costs . . . 59
5.1.5 Gas turbines . . . 59
5.1.6 O shore vs. onshore . . . 59
5.2 Model uncertainties . . . 60
5.2.1 Data . . . 60
5.2.2 Model resolution . . . 60
5.2.3 Software limitations . . . 61
5.3 External uncertainties . . . 62
5.3.1 Alternative products . . . 62
5.3.2 Policy aspects . . . 62
5.3.3 E-fuel market . . . 63
5.4 Societal, ethical and ecological aspects . . . 64

6 Conclusion 65
6.1 Future work . . . 67

Bibliography 69

A Case illustration I
A.1 Grid support case . . . I
A.2 Hydrogen case . . . I
A.3 Ammonia case . . . II

A.4 Methanol case II

B Electrolyzer standby III

C Grid support VII
C.1 Transfer capacity VII
C.2 Battery pro t VIII
C.3 Hydrogen pro t X

D Hydrogen XIII
D.1 Electrolyzer capacity XIII
D.2 Battery operation XV

E Ammonia and methanol XVII
E.1 NH_3 production vs. H_2 containers XIX

List of Figures

1.1 Infrastructure of the energy system, consisting of a 1 GW wind farm, batteries, fuel cells, electrolyzers, hydrogen tanks and production facilities for methanol and ammonia synthesis [14]. 4

2.1 Normalized wind farm production, in the sea outside Skåne in 2019 [32]. 7
2.2 Electricity production from a 1 GW wind farm (green) together with di erent transformer capacities (Upper blue: actual SE4 demand in 2019. Yellow: SE4 2019 with a 1 GW maximum. Lower blue: SE4 2019 with a 500 MW maximum. Red: 500 MW constant.) 9
2.3 Nord pool electricity prices for the SE4 zone in 2019 and 2022 [36, 42]. 10
2.4 Basic principle of a PEM fuel cell. 13
2.5 Polarization curve (grey) and corresponding power density (black), as a function of current density. 13
2.6 Voltage losses in a PEM cell and the resulting polarization curve. . . 14
2.7 Constructing a 6th order polynomial to resemble a typical fuel cell e ciency curve. 17
2.8 Four types of hydrogen storage tanks, type I to type IV from left to right. 19
2.9 UMOE Advanced Composite's type IV hydrogen storage. 20

3.1 System architecture in Odyssey. 28
3.2 Scale factor depending on the hydrogen and methanol storage SoC (Exp_{MeOH} = 0.5 and Exp_{H_2} = 2). 30

4.1 Production and consumption during one year. Allowing electrolyzer standby, minimum production rate = 1,300 kg_{H_2}/h, no battery. Blue ovals mark the time periods when electrolyzers are on standby. (Upper graph in red: wind farm production, green: electrolyzer. Lower graph in red: grid injection.) 33
4.2 Pro t as a function of the supplied electricity (Transfer capacity: 500MW_{peak}). Note: 1,000 batteries correspond to 307 MWh. 37
4.3 Pro t as a function of the supplied electricity (Electrolyzer: 250MW. Fuel cell: 250MW. Transfer capacity: 500MW_{peak}). Note: 50 hydrogen containers correspond to 63 $tons_{H_2}$. 38
4.4 Total amount of hydrogen produced and electricity supplied vs. electrolyzer capacity (Transfer capacity: unlimited). 41

4.5 Profit from hydrogen production over the total system lifetime, as a function of electrolyzer capacity, for different market prices and investment costs. Compared to a traditional grid support case, see Table 4.1, which constitutes a profit baseline by which the other cases can be compared. (Transfer capacity: unlimited. Electricity price: SE4 2019). 41

4.6 Profit from hydrogen production over the total system lifetime, as a function of electrolyzer capacity, for different market prices and investment costs. Compared to a traditional grid support case, see Table 4.1, which constitutes a profit baseline by which the other cases can be compared. (Transfer capacity: unlimited. Electricity price: SE4 2022). 42

4.7 Profit from hydrogen production over the total system lifetime, as a function of electrolyzer capacity, for different market prices and investment costs. Compared to a traditional grid support case, see Table 4.1, which constitutes a profit baseline by which the other cases can be compared. (Transfer capacity: unlimited. Electricity price: SE4 2022. Hydrogen market price: 8.5 vs. 9.5 €/kg$_{H_2}$). 43

4.8 NH_3 production and electricity supplied vs. the number of hydrogen containers, with a 26 tons$_{NH_3}$/h production rate and 250 MW electrolyzer. (Transfer capacity: unlimited. Electricity price: SE4 2019.). 47

4.9 Profit from NH_3 production over the total system lifetime, as a function of the NH_3 production rate and at a constant hydrogen storage and electrolyzer capacity. (Transfer capacity: unlimited. Electricity price: SE4 2019. Market price: 1,000 €/ton$_{NH_3}$). 47

4.10 Profit from MeOH production over the total system lifetime, as a function of the MeOH production rate, with a 500 MW electrolyzer and 15 hydrogen containers. (Transfer capacity: unlimited. Electricity price: SE4 2019. Market price: 400, 600, 800 and 1,500 €/ton$_{MeOH}$). 48

4.11 Profit from MeOH production over the total system lifetime, as a function of the number of hydrogen containers, with a 100 MW electrolyzer and a rate of 10,000 kg$_{MeOH}$/h. (Transfer capacity: unlimited. Electricity price: SE4 2019. Market price: 600 and 1,500 €/ton$_{MeOH}$). 49

4.12 Profit from MeOH production over the total system lifetime, as a function of the number of hydrogen containers, with a 400 MW electrolyzer and a rate of 39,000 kg$_{MeOH}$/h. (Transfer capacity: unlimited. Electricity price: SE4 2019. Market price: 600 and 1,500 €/ton$_{MeOH}$). 50

4.13 MeOH production and electricity supplied vs. the number of hydrogen containers, with a 39 tons$_{NH_3}$/h production rate and 400 MW electrolyzer. (Transfer capacity: unlimited. Electricity price: SE4 2019.). 50

4.14 Profit from NH_3 production over the total system lifetime, as a function of electrolyzer capacity, for different market prices. Compared to a traditional grid support case, see Table 4.1, which constitutes a profit baseline by which the other cases can be compared. (Transfer capacity: unlimited. Electricity price: SE4 2019. Market price: 450, 1,000 and 1,500€/ton$_{NH_3}$). 51
4.15 Profit from MeOH production over the total system lifetime, as a function of electrolyzer capacity, for different market prices. Compared to a traditional grid support case, see Table 4.1, which constitutes a profit baseline by which the other cases can be compared. (Transfer capacity: unlimited. Electricity price: SE4 2019. Market price: 400, 600 and 800€/ton$_{MeOH}$). 52
4.16 Profit from NH_3 production over the total system lifetime, as a function of electrolyzer capacity, for different market prices. Compared to a traditional grid support case, see Table 4.1, which constitutes a profit baseline by which the other cases can be compared. (Transfer capacity: 500MW$_{constant}$. Electricity price: SE4 2019. Market price: 450, 1,000 and 1,500€/ton$_{NH_3}$). 53
4.17 Profit from MeOH production over the total system lifetime, as a function of electrolyzer capacity, for different market prices. Compared to a traditional grid support case, see Table 4.1, which constitutes a profit baseline by which the other cases can be compared. (Transfer capacity: 500MW$_{constant}$. Electricity price: SE4 2019. Market price: 400, 600 and 800€/ton$_{MeOH}$). 53
4.18 Recommended e-fuel to produce, along with the highest achievable profit compared to the grid injection baseline (Transfer capacity: Unlimited. Electricity price: SE4 2019) 55

A.1 The energy system with grid support prioritized, optional battery, electrolyzer and fuel cell [14]. I
A.2 The energy system with hydrogen production prioritized, optional grid support [14]. I
A.3 The energy system with NH_3 production prioritized, optional grid support [14]. II
A.4 The energy system with MeOH production prioritized, optional grid support [14]. II

B.1 Allowing electrolyzer standby, minimum production rate = 1,300 kg$_{H_2}$/h, no battery. (Upper graph in red: wind farm production, green: electrolyzer. Lower graph in red: grid injection.) III
B.2 No electrolyzer standby, minimum production rate = 1,300 kg$_{H_2}$/h, no battery. (Upper graph in red: wind farm production, green: electrolyzer. Lower graph in red: grid injection, blue: grid extraction.) . . IV
B.3 Allowing electrolyzer standby, minimum production rate = 0 kg$_{H_2}$/h, no battery. (Upper graph in red: wind farm production, green: electrolyzer. Lower graph in red: grid injection.) IV

B.4 Allowing electrolyzer standby, minimum production rate = 1,300 kg_{H_2}/h, battery added. (Upper graph in red: wind farm production, green: electrolyzer. Lower graph in red: grid injection.) V

B.5 No electrolyzer standby, minimum production rate = 1,300 kg_{H_2}/h, battery added. (Upper graph in red: wind farm production, green: electrolyzer. Lower graph in red: grid injection, green: battery discharge.) V

B.6 Allowing electrolyzer standby, minimum production rate = 0 kg_{H_2}/h, battery added. (Upper graph in red: wind farm production, green: electrolyzer. Lower graph in red: grid injection.) VI

C.1 Transfer capacity: Unlimited / Actual SE4 VII

C.2 Transfer capacity: $1GW_{peak}$ VII

C.3 Transfer capacity: $500MW_{constant}$ VIII

C.4 Transfer capacity: $500MW_{peak}$ VIII

C.5 Pro t as a function of the number of batteries (Transfer capacity: $1GW_{peak}$). IX

C.6 Pro t as a function of the number of batteries (Transfer capacity: $500MW_{constant}$). IX

C.7 Pro t as a function of the number of batteries (Transfer capacity: $500MW_{peak}$). X

C.8 Electrolyzer and fuel cell operating to support the grid (Electrolyzer: 150MW. Fuel cell: 50MW. Transfer capacity: $500MW_{peak}$). XI

C.9 Electrolyzer and fuel cell operating to support the grid (Electrolyzer: 100MW. Fuel cell: 100MW. Transfer capacity: $500MW_{peak}$). XI

C.10 Electrolyzer and fuel cell operating to support the grid (Electrolyzer: 250MW. Fuel cell: 250MW. Transfer capacity: $500MW_{peak}$). XII

D.1 Resulting grid injection (rst graph, blue), electricity and hydrogen incomes (second graph, blue and green resp.), and wind power utilization (third graph, red) for a 250 MW electrolyzer (Transfer capacity: unlimited). XIII

D.2 Resulting grid injection (rst graph, blue), electricity and hydrogen incomes (second graph, blue and green resp.), and wind power utilization (third graph, red) for a 500 MW electrolyzer (Transfer capacity: unlimited). XIV

D.3 Resulting grid injection (rst graph, blue), electricity and hydrogen incomes (second graph, blue and green resp.), and wind power utilization (third graph, red) for a 750 MW electrolyzer (Transfer capacity: unlimited). XIV

D.4 Electrolyzer operating with 0 batteries (Grid injection: disabled). . . XV

D.5 Electrolyzer operating with 1,000 batteries (Grid injection: disabled). XV

D.6 Electrolyzer operating with 10,000 batteries (Grid injection: disabled).XVI

E.1 Resulting NH_3 production rate and H_2 storage SOC (upper graph, blue and red resp.), along with wind power utilization (lower graph, red) and electrolyzer power consumption (lower graph, green) for a 250 MW electrolyzer (Transfer capacity: unlimited). XVII
E.2 Resulting MeOH production rate and H_2 storage SOC (upper graph, blue and red resp.), along with wind power utilization (lower graph, red) and electrolyzer power consumption (lower graph, green) for a 250 MW electrolyzer (Transfer capacity: unlimited). XVIII
E.3 Resulting NH_3 production rate and H_2 storage SOC (upper graph, blue and red resp.), along with wind power utilization (lower graph, red) and electrolyzer power consumption (lower graph, green) for 46 H_2 containers (Transfer capacity: unlimited). XIX
E.4 Resulting NH_3 production rate and H_2 storage SOC (upper graph, blue and red resp.), along with wind power utilization (lower graph, red) and electrolyzer power consumption (lower graph, green) for 300 H_2 containers (Transfer capacity: unlimited). XIX

List of Tables

2.1 Wind farm parameters used in this study. 7
2.2 Battery parameters used in this study. 12
2.3 Electrolyzer parameters used in this study. 16
2.4 Fuel cell parameters used in this study. 18
2.5 Stationary storage tank parameters (Type IV, composite breglass, 1 container) used in this study. 20
2.6 Ammonia synthesis parameters used in this study. 22
2.7 Methanol synthesis parameters used in this study. 25
2.8 Economical parameters used in this study. 26

3.1 Controller algorithms used in this study. 29

4.1 Electricity sales income, pro t and payback time (PBT) for di erent electricity prices. 35
4.2 Electricity supplied, pro t and PBT for di erent transfer capacities. . 35
4.3 Grid support case: peak-load shifting con guration. 36
4.4 Resulting amount of electricity supplied to the grid, investment cost, and payback time (PBT), when maximizing the pro t from the addition of batteries to the grid support case for di erent grid transfer capacities. 37
4.5 Resulting amount of electricity supplied to the grid, investment cost, and payback time (PBT), when maximizing the pro t from the addition of fuel cells and electrolyzers to the grid support case (Electricity price: SE4 2022. Transfer capacity: 500MW_{peak}). 38
4.6 Comparison of traditional grid support and pro t-maximized peak-load shifting scenarios, considering utilized wind energy (UWE), amount of electricity supplied to the grid, and investment cost (Electricity price: SE4 2022. Transfer capacity: 500MW_{peak}). 39
4.7 Hydrogen case: battery addition con guration. 43
4.8 Comparison of technical and economic characteristics of NH_3 and MeOH production. 45
4.9 Ammonia and methanol case con guration. 45
4.10 Optimized number of hydrogen storages for di erent combinations of electrolyzer capacities and NH_3 production rates (NH_3 market price: 1,000 ¿/ton $_{NH_3}$. Electricity price: SE4 2019. Transfer capacity: Unlimited). 48

4.11 Optimized numbers of hydrogen containers for di erent combinations of electrolyzer capacities and MeOH production rates (MeOH market price: 600 ¿/ton $_{MeOH}$. Electricity price: SE4 2019. Transfer capacity: Unlimited). 51
4.12 Recommended e-fuel to produce, along with the highest achievable pro t compared to the grid injection baseline (see Figure 4.5, 4.14 and 4.15), for various market price combinations given in ¿/kg $_{H_2}$, ¿/ton $_{NH_3}$ and ¿/ton $_{MeOH}$. (Transfer capacity: unlimited. Electricity price: SE4 2019). 54

B.1 System con guration when evaluating the technical behaviour of electrolyzer standby. III

C.1 Resulting investment cost, electricity supplied to the grid, pro t and PBT for di erent numbers of batteries (Transfer capacity: 1GW$_{peak}$). VIII
C.2 Resulting investment cost, electricity supplied to the grid, pro t and PBT for di erent numbers of batteries (Transfer capacity: 500MW$_{constant}$). IX
C.3 Resulting investment cost, electricity supplied to the grid, pro t and PBT for di erent numbers of batteries (Transfer capacity: 500MW$_{peak}$). X
C.4 Investment cost, amount of electricity supplied to the grid, pro t and payback time (PBT) varying with the number of hydrogen storage containers (Electrolyzer: 250MW. Fuel cell: 250MW. Transfer capacity: 500MW$_{peak}$). X

1

Introduction

Climate change has become a global issue often mentioned in the news and media. A recent ambition to slow down the rising temperatures is the Paris Agreement, a global agreement consisting of rules and guidelines with the final aim of staying far below a 2°C increase of the global average temperature [1]. To accomplish this and hopefully also stay within a 1.5°C increase, all use of fossil fuels needs to be reduced or even completely terminated while simultaneously achieving negative emissions to decelerate global warming even more. This has led to the major trend of electrification predominantly in sectors such as industry and transportation [2]. According to the Swedish Energy Agency's (SEA) forecast Sweden's electricity demand will increase from a yearly demand of 140 TWh_{el} today, to around 280 TWh_{el} by the year 2035. Combined with this forecast they suggest that a large part of the needed increase in production could come from offshore wind farms, given that it would be techno-economically feasible. The overall feasibility is not only affected by economic parameters but also the irregular variations in power generation that come with intermittent renewable energy sources (RES) such as wind power [3].

Intermittent energy sources are expected to have a more significant role in the future, which is why it is of great importance to evaluate how these variations can be managed to reduce the strain on the grid [2, 3]. Given the right tools companies and prosumers (electricity consumers that also produce electricity) can even benefit economically from these variations by for example adapting an industrial process to when the electricity price is high or low, or by selling and buying electricity utilizing an energy storage such as a battery [4]. More recent methods on how to make use of the variations in a future electricity grid have also emerged, some of which will be evaluated in this study. That is, as a complement to the core business of wind farms, which is to supply the grid with renewable electricity, the electricity can be used to produce hydrogen, using electrolyzers [5]. Produced hydrogen can thereafter either be used in a fuel cell to produce electricity when there is a lack of wind or sold to the hydrogen market (e.g. as a fuel for transport or as feedstock to chemical industries).

Another option for wind farm owners is to use hydrogen to produce chemical products of potentially higher value, for example, so-called e-fuels (also known as e.g. electrofuels, synthetic fuels, and power-to-x) [6]. A key condition for e-fuels is that they have to be a product of electricity, water, and often carbon dioxide (CO_2) or nitrogen (N_2) captured either from the air or from a concentrated source. Just as the name e-fuels suggests, electricity has to be the primary source of energy during production. If the electricity and CO_2/N_2 would also come exclusively from renewable sources, these e-fuels could be completely climate neutral as they don't add or extract any new CO_2 emissions to the environment. E-fuels have this far demonstrated a lot of potential for the transportation sector such as a simple adoption of them in our existing infrastructure as well as allowing for signi cant reductions of CO_2 emissions. Three common e-fuels that will be investigated in this study are hydrogen, methanol and ammonia, as studies often nd these compounds to be most cost-e ective compared to alternative e-fuels [7, 8, 9, 10].
The alternative to producing e-fuels, which is to store hydrogen for the purpose of generating electricity when there is a lack of wind, comes with a cost since the total e ciency of going from electricity to hydrogen and back to electricity again is typically around 33% [11]. Therefore there may be alternative strategies that are techno-economically reasonable for companies, combining supplying electricity to the grid and producing electrofuels in the process.

The trend of electri cation will most likely play a prominent role when trying to uphold the Paris Agreement, given that produced electricity doesn't result in signi cant greenhouse gas emissions. According to the International Energy Agency (IEA), roughly 29% of the world's electricity generation came from RES in 2021 and can be considered green, which in extension means that electrifying the industry and transportation sectors would result in signi cant CO_2 emissions given that most electricity still comes from fossil fuels [12]. In addition to electri cation another approach to reduce CO_2 emissions is the transition from fossil fuels to e-fuels, which is why this study's subject is of foremost importance.
There is still research left to be done when it comes to comparing the techno-economical feasibility of di erent e-fuels [6]. Production of fossil equivalents is likely less restrained since heat and electricity are abundantly available from the grid or connected processes. E-fuels are preferably a product of RES, which results in less reliable production due to the intermittency. The production is further aggravated if the additional condition of supplying electricity to the grid is factored in. This is why energy systems modelling connected to e-fuel production as a subject is especially interesting and important for the world's future energy infrastructure.

1.1 Aim

The aim of this study was to techno-economically model and evaluate how an e-fuel production site performs under di erent conditions when connected to an o shore wind farm. This was done using the software Odyssey from Seed Energy, which is designed for modelling complex energy systems to asses technical, economic and environmental parameters. Conclusions are drawn regarding important parameters and the main goal was to provide recommendations regarding how certain units should be run and which investments are most critical for the overall technical feasibility.
The following research questions are evaluated:
Q1. Which are the most important parameters to consider before investments to ensure a techno-economically feasible e-fuel-producing energy system?
Q2. How are di erences in the production method of di erent e-fuels a ecting the overall performance and exibility of the energy system?
Q3. How are market prices a ecting the pro tability of producing hydrogen, ammonia and methanol?
Q4. What does peak-load shifting with batteries and hydrogen provide to the energy system?
Q5. Why is hydrogen storage a necessary part of the studied energy system? How is the technical and economic performance a ected?
Q6. How can Odyssey be used to evaluate similar energy systems?

1.2 Methodology

The thesis implies that extensive modelling and analysis of an o shore wind farm connected to an e-fuel production site is carried out. Three cases were assumed from which the main analysis proceeded. These cases consist of a 1 GW wind farm that can provide electricity to an e-fuel production site and to the electrical grid as shown in Figure 1.1. The energy system was assumed to be located in the electricity bidding area referred to as zone SE4 in Sweden (Nord Pool, 2020) [13]. The analysis is primarily based on the decision-making connected to such an energy system to ultimately be able to draw scienti c conclusions and give recommendations regarding investments in the perspective of producing hydrogen, ammonia or methanol. To further nuance the analytical and scienti c part of the thesis, di erent objectives were used to broaden the results and expectedly produce some interesting insights. The scenarios could for example involve supporting the grid with fuel cells and batteries or comparisons of di erent transformer capacities. Consequently, only a few of all the possible combinations of case and scenario were evaluated due to a short time frame. Further combinations and evaluations are therefore left for future studies.

Figure 1.1: Infrastructure of the energy system, consisting of a 1 GW wind farm, batteries, fuel cells, electrolyzers, hydrogen tanks and production facilities for methanol and ammonia synthesis [14].

2

Theoretical background

2.1 Variational Management Strategy

Today's energy infrastructure can experience many di erent variations in both loads and prices for energy sources such as electricity and heat. These variations can be diurnal, weekly or even yearly depending on behaviors in both production and usage, as well as climate and weather. Typical diurnal variations could be when households decrease their electricity demands at night, while a typical seasonal variation is an increase in both heat and electricity demand during winter time. Electricity systems without RES typically only experience human-induced diurnal variations, and these are managed by employing peak-producing units such as gas and oil- red ones [15, 16]. In contrast, wind and solar generation can further complicate the task of supplying electricity demands as they can lead to large de cits for some hours as well as large surpluses at other hours, making it crucial for other power generation units in the grid to be exible and operate accordingly. Since the SEA suggests that a large part of the upcoming expansion of electricity production in Sweden can come from wind power, much larger and more irregular variations in the power grid should be expected [2]. Thus, the principle of variational management strategy (VMS) has become progressively more central.

A VMS is used to handle certain variations in the power system to ensure that the amount of produced electricity is equivalent to the amount consumed [3]. VMSs are frequently used in combination as they address di erent behaviors, and thus the result is improved if combined successfully. The VMS that will be employed in this study is peak-load shifting, by using batteries and hydrogen production. Batteries and hydrogen storage can be used to store energy when a wind farm is overproducing and return the stored energy when the grid is experiencing de cits. These strategies work similarly but with a signi cant di erence in the time of storage. Batteries have the major drawback of storage degradation over time, which in extension implies that they are best suited for short-term energy storage. Hydrogen is stored in a tank and is thus not prone to exhibit the same disadvantage. The reason why peak-load shifting is important when deploying large-scale wind farms is to counteract and respond to the variations wind power implies. By doing that, the operational exibility of the overall system can be increased, which in extension suggests that the concept of complete carbon neutrality is technically viable.

2.2 O shore large-scale wind farm

Wind energy can be transformed into electricity in a lot of ways, but the most mature and well-known process is by using horizontal axis wind turbines. These turbines consist of a tower, generator housing (nacelle) and most often three rotor blades [20]. When the wind hits the blades and the turbine starts rotating, wind energy is transformed into electricity. The resulting power output can be calculated according to Equation 2.1, where P is the potential power and V_{wind} is the wind speed [21]. In that equation, it can be seen that the power output is a product of V_{wind}^3, which tells us that wind speed is a crucial parameter when producing electricity. Because wind speeds increase with height, as displayed in Equation 2.2, the length of the tower is another crucial parameter for wind production [17].

$$P = \frac{A \ C_p}{2} \ V_{wind}^3 \tag{2.1}$$

$$\frac{V_h}{V_r} = \frac{H_h}{H_r}^{Y} \tag{2.2}$$

In Equation 2.2, V_h is the average wind speed at hub height H_h, V_r is the wind speed at reference height H_r, and Y is the power exponent, illustrating that an increased hub-height, results in an increased wind speed. Furthermore, by utilizing the "large-scale wind farm"-concept, geographical smoothening can result in a larger and more stable electricity production [18]. Irregularities in wind speeds become less emphasized and the so-called wind speed probability distribution tends to be higher, which in simple terms means that the average wind speeds will be higher and thus produce more electricity [19]. Moreover, the placement of the wind farm can also play a signi cant role in the resulting electricity production.

2.2.1 Wind farm characteristics

The energy system is assumed to be located o shore, in the Swedish bidding area called SE4, with a maximum power output of 1 GW. Typically wind turbines' production capacity is decreasing over time, and a study in 2014 based on 282 wind turbines in the UK, and a total of 1686 hours, found this decrease to be 1.6–2.2% per year of the initial capacity [22]. It is worth noting that they concluded more research could be done to determine whether the production decrease is linear, quadratic or logarithmic. In this study, however, an annual production decrease rate of 1.6 %/year is assumed.

The initial investment cost of the energy system will not a ect results concerning the pro tability of di erent operational strategies, but foremost factors such as nal payback times. Since this study has its main focus on operating a wind farm with an e-fuel production site and energy storage system, investment costs can be disregarded. In the case of curiosity towards more general investment decisions, however, an investment cost of 2,700 €/kW will be assumed. In the case of curiosity towards more general investment decisions, an investment cost of 2.7 M€/MW will be assumed. This assumption is based on a guide to o shore wind farms given by the organisation BVG Associates (with a currency conversion rate of 0.94 €/$) [23].

This cost can be veri ed by other studies claiming costs of similar values [24, 25]. The latter study also describes that there has been a learning curve during the past years, giving a reason for why the investment cost can vary between 2 and 4 M¿/MW. The cost can also be reconsidered and adjusted later on if necessary, by comparing parameters such as payback times to real cases. Studies indicate that a typical payback time should be around 4-7 years, but could go as high as 11-13 years [26, 27, 28, 29].
In this study, an annual O&M (Operations and maintenance) cost of 2% of the investment cost is assumed, as this value is frequently seen in similar studies [30, 31].

Table 2.1: Wind farm parameters used in this study.

Parameter	Value	Unit	Reference
Production capacity	1000	MW	Assumption
Annual production decrease rate	1.6	$\%_{capacity}$/year	[22]
Investment cost	2700	M€	[23, 24]
Annual O&M cost	2	% of total inv.	[30, 31]

The website called Renewables.ninja is used for hourly o shore wind production data, as the site has the option of choosing the location along with commercial wind turbine, turbine height, capacity and year [32]. In this study, the Siemens SWT 4.0 130 was assumed, as its height of 90 meters and the large swept area is assumed to be well suited for o shore production [33]. The location was set to the eastern shore of Skåne (Lat: 55.77, Lon: 15.05) as there are, according to Skånes vindkraftsakademi and Energimyndigheten, future plans to build an o shore wind park there [34, 35]. The wind production data, for the year of 2019, is illustrated in Figure 2.1.

Figure 2.1: Normalized wind farm production, in the sea outside Skåne in 2019 [32].

2.3 Power grid

A power grid is an interconnected network of substations, power grid equipment and transmission lines [37]. Larger substations are often placed close to electrical producers, while smaller ones tend to be closer to the consumer. The reason for this is connected to the voltage at which the electricity is transferred. Increasing the voltage typically results in reduced losses of electricity transfer, and the voltage can vary from 230 V to 275 kV. In Sweden, the grid can be divided into two subgroups; transmission grid and distribution grid [38]. The transmission grid's voltage varies between 220-400 kV depending on what distance the electricity is transferred, while the distribution grid's voltage handles all the lower voltages down to 230 V which is used in household outlets.
Substations can be comprised of equipment handling power quality and frequency such as inverters, recti ers and capacitors, but also safety equipment such as circuit breakers [37]. A substation's main purpose, however, is most often to transform the in-going voltage, consequently leading to transformers being a crucial component. Traditionally, transformers and transmission lines have been operated with a static thermal rating based on "worst-case conditions", neglecting dynamic thermal e ects during operation, known as static line rating (SLR) and static transformer rating (STR) [39]. This can in an energy system, result in wind power curtailment due to thermal limitations. By instead introducing dynamic ratings for the lines (DLR) and transformers (DTR) taking heat balances with weather conditions into account, more e cient utilization of the transmission system can be achieved. A study in 2022 comparing combinations of static and dynamic ratings, found that simultaneous use of DLR and DTR could reduce wind energy curtailment down to zero while also reducing operational costs, by taking real-time capacities into account. By assuming that lines and transformers are dynamically operated and also over-dimensioned, limitations connected to electricity transmission can be disregarded. This can be further enforced since the theoretically acceptable maximum from o shore sites, according to the Swedish Transmission System Operator (TSO), is around 1.8-2 GW [40]. Additionally, currently developing wind farm areas will have a minimum of 1.4 GW transfer capacity, which is well enough higher than the planned 1 GW wind farm output.
The distance of transmission impacts what type of transformer station is needed and also the associated investment costs. High voltage direct current (HVDC) stations are for example commonly used for transmission at longer distances, as a higher voltage with direct current (DC), rather than alternating current (AC), is known to minimize long-distance transmission losses [41].

2.3.1 Power grid characteristics

Transmission losses and limitations are assumed to be neglected in this study. In a realistic case, the actual transmission losses could be compensated for by simply reducing what is considered to be the maximum production capacity. By disregarding transfer losses from the wind farm to the production site or electricity grid, we also disregard the wind farm's distance to land.

As it is ideal for this study to consider the wind farm as a varying source of electricity, and the grid as a varying demand of electricity, equipment responsible for power quality and frequency will be disregarded. Nevertheless, transformers and transmission lines can still have a signi cant impact on the nal evaluations. When evaluating the energy system's ability to support the grid, di erent limits of transmission between the grid and the wind farm can be compared, as shown in Figure 2.2. Using the total demand of electricity bidding zone SE4 as a limit will have the same e ect as an unlimited transfer capacity. The SE4 demand can further be scaled to simulate the demand of an isolated area or region, also called a microgrid. In this study, the SE4 demand is scaled to have a maximum of 1 GW (denominated $1GW_{peak}$) and 500 MW (denominated $500MW_{peak}$). Together with those transfer capacities, a constant 500 MW limit (denominated $500MW_{constant}$) will also be evaluated. The ramp-up rate of electricity extractions and injections is assumed to be the same capacity as the maximum power itself, thus neglecting limitations associated with dynamics in the transformer. The expenditures of the power grid connection are assumed to be included in the wind farm's investment and O&M cost.

Figure 2.2: Electricity production from a 1 GW wind farm (green) together with di erent transformer capacities (Upper blue: actual SE4 demand in 2019. Yellow: SE4 2019 with a 1 GW maximum. Lower blue: SE4 2019 with a 500 MW maximum. Red: 500 MW constant.)

An open-source data platform called Open Power System Data is used to acquire hourly data for electricity grid demands and prices for the SE4 area during 2019, as seen in Figure 2.2 and 2.3 respectively [36]. Additionally, Vattenfall's database was also used to acquire more recent electricity prices, as also seen in Figure 2.3 [42].

Figure 2.3: Nord pool electricity prices for the SE4 zone in 2019 and 2022 [36, 42].

It is evident that the prices of 2022 were much higher than during 2019, which likely will have a large impact on economic parameters such as pro t and payback time. Additional fees that could be associated with electricity prices and power transmissions, such as injection and subscription fees, green incentives and TSO tari s are neglected in this study.

2.4 Batteries

An electrochemical cell is per de nition a cell by which energy is transformed between the states of electricity and chemical energy [43]. Batteries can utilise electrochemical energy conversion reversibly with for example Li-ions to allow several cycles of charging and discharging. This conversion is e cient and fast, proving itself ideal for electrical applications such as smartphones and more recently cars. As with any chemical reaction, there are several factors that a ect the general performance of batteries. State of charge (SoC) and depth of discharge (DoD) are some of the parameters that have been shown to have a signi cant impact on a battery's lifetime [44, 45]. For example, operating a battery at a lower DoD has been shown to prolong its lifetime [45, 46]. Furthermore, centering the DoD around 50% (e.g. 10-90% or 40-60%) can have an even more substantial e ect on capacity degradation. Another important factor for a battery's lifetime is its C-rate, which is the rate at which a battery is fully discharged relative to its maximum capacity. A battery with a C-rate of 1C means that it can be fully discharged in one hour, 2C in 30 minutes, and 0.5C in 2 hours. Combining a lower DoD with a lower C-rate tends to result in a lower rate of capacity degradation according to [47], where studies on commercially available batteries were summarized. To further minimize capacity degradation the batteries could be cycled around a SoC of 50%, thus avoiding both the highest and lowest percentages.

On top of capacity degradation, which indicates a decreasing maximum storage capacity over time, self-discharge causes the SoC to decrease over a temporary time span [48]. The self-discharge rate is predominantly a ected by the battery system's use of auxiliaries for cooling/heating and control units etc. Due to self-discharge, it can be proved ine cient to use batteries to cover electricity demands during longer periods with a lack of wind. Overinvesting in a signi cantly larger battery to store large amounts of energy over a few days, but ending up losing that energy due to self-discharge, would likely not be a techno-economically viable option in a system such as the one studied in this study. Batteries are instead ideal for shorter periods of storage.

2.4.1 Battery characteristics

The electrical storage used in the energy system is assumed to be a Li-ion battery. Characteristics are summarized in Table 2.2, and include for example e ciency and capacity degradation. Several values are gathered from what studies claim as reasonable, while other parameters might be of a more theoretical nature. Therefore, a commercially available battery from Tesvolt named "TS HV 70 OUTDOOR" is also used for reference [49]. Their battery uses several lithium NMC cells from Samsung SDI, who claims that each cell has a minimum of 80% of its initial capacity after 6,000 cycles [50]. This implies that the cell capacity degrades at a maximum rate of 0.003%/cycle, which is assumed for this study. With the Tesvolt as a reference, we also assume an e ciency of 98%. Lithium NMC is an abbreviation for Lithium-Nickel-Manganese-Cobolt ($LiNi_{0:5}Mn_{0:3}Co_{0:2}O_2$), which is used as cathode in such batteries. A study evaluating this cathode recommends using a SoC interval between 30-70% [51]. The study also suggests that NMC batteries might bene t from higher C-rates. Another study reports that a strictly constant operating temperature will make battery ageing less a ected by the C-rate [47]. In this study, the Tesvolt C-rate of 1C is assumed, as well as a constant operating temperature [49].

The Tesvolt's size of 307 kWh will be used as a reference point when modelling [49]. The appropriate number of batteries utilised in the energy system will be decided from evaluation and optimization depending on strategy and case. It is important to note that the DoD corresponds to the storage capacity, as the usable storage of a 100 kWh battery with a DoD=1 equals 200 kWh capacity with a DoD=0.5. The battery will in this study be cycled with a DoD of 0.8, in the interval 10-90%. Since a lower DoD can extend a battery's lifetime, a larger storage capacity with a lower DoD could postpone battery replacement. This trade-o will however be disregarded in this study, as evaluating e-fuel production is seen as more important. The self-discharge rate is assumed to be 0.016 %/day, as a study found that Li-ion batteries rarely discharge more than 5% over 1 month [48]. The cost of the Tesvolt battery is unknown. The general cost, however, based on BloombergNEF's annual price survey, was 142 €/kWh (151 $/kWh) in 2022 [52]. This cost increased compared to the previous year, perhaps due to shutdowns caused by covid-19, but the cost is according to BloombergNEF expected to fall below 94 €/kWh (100 $/kWh) in 2026. An O&M cost of 1% is assumed, as a study suggests that 1% is a frequently recurring value [53], and is assumed for this study.

As the data sets presented in Section 2.3.1 have hourly time steps, technical parameters with a higher resolution, such as maximum charge power increase rate, are disregarded in this study. A battery's ramp-up and ramp-down rates tend to be on a second or minute basis, which means that ramping up or down a battery's power in- or output to the maximum limit would occur within one time-step in the model [54].

Table 2.2: Battery parameters used in this study.

Parameter	Value	Unit	Reference
Capacity	307	kWh	[49]
SoC interval	10-90	%	Assumption
Charge & discharge e ciency	98	%	[49]
C-rate	1C	-	[49]
Self-discharge rate	21.32	$Wh/h_{absolute}$	[48]
Capacity degradation	0.0092	Wh/cycle	[49, 50]
Investment cost	142	¿/kWh	[52]
Annual O&M cost	1	% of total inv.	[53]

2.5 Proton exchange membrane

Batteries are not the only modern instance of electrochemical energy conversion. More recent concepts that have already been mentioned in this study are fuel cells and electrolyzers. There are several types of cells where di erent reactions occur, three well-known ones being the alkaline, solid oxide and proton exchange membrane cells. The reaction of the latter cell mentioned, also known as a PEM cell, is illustrated by Equation 2.3. The main advantages of PEM cells are their maturity, fast dynamics and cold-start capability [66]. These bene ts will in extension result in very high operational exibility that is preferred in an infrastructure such as the energy system studied in this study. Due to these advantages, the PEM cell is the only type of cell considered in this study. A PEM cell consists of two gas di usion electrodes (cathode and anode), catalyst, membrane and ow eld plates, as illustrated in Figure 2.4 [58]. What separates the anode and cathode in a PEM cell is as the name suggests a membrane that has been carefully engineered to only let protons through. This combined with an electrical conductor between the cathode and anode gives rise to a voltage potential and by extension, a current. Note that the reaction is bidirectional, allowing the production of either hydrogen (electrolyzer) or electricity (fuel cell) [76].

$$H_2O \quad 2H^+ + 2e^- + \frac{1}{2}O_2 \quad H_2 + \frac{1}{2}O_2 \tag{2.3}$$

Figure 2.4: Basic principle of a PEM fuel cell.

Two important parameters when characterizing a fuel cell are current density and cell voltage, often given with a polarization curve, see Figure 2.5 [59, 64]. A polarization curve illustrates the relation between voltage (V) and current (I) in a fuel cell, and can suggest at what current the maximum power (P) of a cell can be achieved using Equation 2.4.

Figure 2.5: Polarization curve (grey) and corresponding power density (black), as a function of current density.

$$P = U \cdot I = [V] \cdot [A/cm^2] = [W/cm^2] \tag{2.4}$$

The highest theoretical voltage that can be attained from a single cell, calculated using Equation 2.5, is 1.23V and is usually referred to as a fuel cell's standard potential [59]. In Equation 2.5, ΔG° is Gibbs free energy at standard conditions (ΔG° = -229 kJ/mol), F is Faraday's constant (F=96,485 C/mole), n is the number of moles of electrons in the reaction (n=2), and E° is the voltage potential at standard conditions, hence called "standard potential".

$$\frac{\Delta G^\circ}{nF} = E^\circ = 1.23V \tag{2.5}$$

The standard potential, however, is practically unattainable due to primarily three types of losses/resistances illustrated in Figure 2.6 [59]. Activation losses can be described as a voltage needed to drive the reaction and tends to a ect the cell potential most signi cantly [64]. Ohmic losses are caused by resistances associated with the electrodes and are proportional to the current density. Concentration losses occur as a result of a decreasing concentration of reactants at the surface of the electrodes and are a ected by current density and electrode structure. Considering these losses, the appearance of the polarization curve is quite reasonable. It is initially decreasing due to activation losses and is gradually being more a ected by the increasing current density. This also explains why optimizing the operating conditions of a PEM cell is so crucial.

Figure 2.6: Voltage losses in a PEM cell and the resulting polarization curve.

Operating a PEM cell at an e cient rate can be di cult due to the complexity of the chemical reaction occurring. The relatively short life span of today's cells can become a barrier to their commercialization, making it crucial to optimize the operational conditions and extend their life [63]. Certain types of cells operate optimally at di erent temperatures and pressures, and factors such as relative humidity and reaction stoichiometry also play a signi cant role during operation [76, 56]. After a PEM cell's operational lifetime, degradation on for example the catalyst, gas di usion layers, and membranes have had a signi cant impact on the systems voltage output. A single cell will typically experience a voltage degradation of between 2-10 $\mu V/h$ over its lifetime [60, 63]. However, in cases where the relative humidity has been too low resulting in dehydrating operating conditions, degradation could go as high as $120 \mu V/h$. A study found that the ohmic losses at high current densities (>1 A/cm^2) could cause the di usion on the cathode and membrane to be insu cient to maintain a hydrated membrane [61]. Optimizing the air stoichiometry in a fuel cell can also have a signi cant impact by reducing the power needed in for example the air compressor [62].

A complication often associated with PEM electrolyzers is the effect of seawater on the cells, most commonly causing degradation of the membranes and catalysts [65]. This degradation occurs mainly due to metallic impurities such as Fe^{3+}, Al^{3+}, Cu^{2+}, Ca^{2+}, Ni^{+} and Na^{+} in the feed water, and typically they have to be limited to a maximum of 0.5 ppm in total [67, 68]. Long-term effects of such impurities causes significantly decreased lifetime and performance of the electrolyzer. To avoid degradation sea water can be treated before entering the cell, ensuring that only high-quality water is used for hydrogen production. This water treatment consists of a desalination and a purification process, whereas the desalination process can be either electrical or thermal. A well-established commercial method is seawater reverse osmosis (RO), which is already used for PEMECs today without significant losses of performance [57, 68]. Due to this fact, and because calculations on thermal streams will be avoided, electrical water treatment with RO is the direct logical choice for the energy system considered in this study.
A PEM cell typically has dynamics fast enough to start and stop within a few minutes, which implies that a model with an hourly resolution won't be able to capture the more technical operations on a minutes or seconds basis [69]. Equivalently to the battery, ramping rates are therefore neglected for the electrolyzer and fuel cell. The possibility of recovering heat is disregarded in this study, and for that reason so is also the thermal properties of a PEM cell. The thermal effects on operational flexibility and efficiency will be accounted for, with an overall efficiency constant for the electrolyzer, and an efficiency curve for the fuel cell (further discussed in 2.5.2).

2.5.1 Electrolyzer characteristics

The efficiency of an electrolyzer can be calculated using Equation 2.6, which gives a percentage based on hydrogen's lower heating value (LHV) [70]. Hydrogen also has a higher heating value (HHV), that if used would result in a lower percentage for the same theoretical efficiency. If the efficiency calculation isn't specified as HHV- or LHV-based, using this equation can lead to misunderstandings. A more accurate way to express the efficiency of an electrolyzer, however, can be to specify the specific energy consumption, in kWh/kg$_{H_2}$, instead. In this study, specific power consumption is most frequently used.

$$\eta_{electrolyzer} = \frac{LHV_{H_2}}{P_{in} = \dot{m}_{H_2,produced}} \tag{2.6}$$

To realistically assume parameters for the electrolyzer operated in this energy system, two commercial PEMECs are used as references. H-TEC systems offers a smaller unit called "ME450", that can produce 18.75 kg$_{H_2}$/h at a nominal power of 1 MW [71]. Siemens Energy offers a larger unit called "Silyzer 300", that can produce 335 kg$_{H_2}$/h at a nominal power of 17.5 MW [72]. They both claim a high dynamic operational flexibility, with ramp-ups and ramp-downs within minutes. Additionally, Siemens has a minimum load of 20% of the total capacity. Since 250 MW corresponds to approximately 14 Siemens Silyzers, the minimum load for the electrolysis in this study is, assuming exactly 14 units are being used, 65 kg$_{H_2}$/h.

The average power consumption of the two references is 52.3 kWh/kg$_{H_2}$ at the beginning of their life (BoL), and 62.2 kWh/kg$_{H_2}$ at the end (EoL). The water used in the PEMEC is desalinated through reverse osmosis as this is found to be a commercially established method, and also a logical choice for this system [68]. The water treatment along with necessary auxiliaries is approximated as an e ciency decrease of 3% of the total e ciency, as suggested in a study [68]. Using Equation 2.6, a 3% e ciency reduction results in a power consumption increase up to 54.9 kWh/kg$_{H_2}$ at BoL and 65.9 kWh/kg$_{H_2}$ at EoL.

Comparing the BoL and EoL power consumptions, and assuming an operational lifetime of 10 years, an e ciency decrease of 1.22e-4 % per hour of operation is attained. This can be validated by studies showing electrolyzer degradation in a range of 1.5-3 µV/h [73, 74]. An average cell voltage of 0.6 (see Figure 2.5 and 2.6) and a decrease of 1.5-3 µV/h would correspond to a percentage decrease of 1.875-3.75 e-4 %/h, i.e. a decrease of the same order of magnitude.

Studies suggest that the investment cost of PEM electrolyzers should be in the range of 963 - 1,576 ¿/kW$_{el}$, but long-term predictions can go as low as 569 ¿/kW$_{el}$ [57]. Di erent investment costs can be used when evaluating the resulting pro ts of the energy system, but the replacement cost after 10 years of operation will be assumed as the lowest one, 569 ¿/kW$_{el}$. The annual costs for O&M are assumed to be 5% of the total investment [75, 76]. The market price of hydrogen varies between 1.3 and 5.5 ¿/kg [57], and this parameter will also be a key result of this study. The price evaluations are important, as the outcome will dictate which e-fuel to especially recommend. For example, one study argued that curtailment of the power produced could be cheaper than producing hydrogen if the hydrogen price was less than 3.7 ¿/kg [57].

Table 2.3: Electrolyzer parameters used in this study.

Parameter	Value	Unit	Reference
Auxiliaries & water treatment	3	% of total e .	[68]
Nominal power consumption (BoL)	54.9	kWh/kg$_{H_2}$	[71, 72]
Nominal power consumption (EoL)	65.9	kWh/kg$_{H_2}$	[71, 72]
Stack nominal power (BoL)	250	MW	Assumption
Stack nominal power (EoL)	320	MW	Calculation
Nominal H_2 production	4,555	kg$_{H_2}$/h	Eq. 2.6
Minimum H_2 production	65	kg$_{H_2}$/h	[72]
E ciency decrease	1.22e-4	%/h$_{operation}$	[71, 72, 73, 74]
Operational lifetime	10	years	Assumption
Investment cost	963 - 1,576	¿/kW	[57]
Replacement cost	569	¿/kW	[57]
Annual O&M cost	5	% of total inv.	[75, 76]
Water cost	0	¿/m^3	Assumption
Hydrogen market price	1.3-5.5	¿/kg$_{H_2}$	[57]

2.5.2 Fuel cell characteristics

Two commercial fuel cells from PowerCell AB are used as references in this study, the "Heavy Duty System 100" and the "Power Generation System 200" [77, 78]. The Heavy Duty System has a rated power output of 100 kW, and a minimum power output of 10 kW. This ratio is assumed for the fuel cell used in the energy system. The Heavy Duty System also has an efficiency of 55% at rated power (BoL), and 45% at peak power (BoL). This efficiency is similar to the Power Generation System's 54% at its rated power. PowerCell claims an operational lifetime of 20,000 hours for the Heavy Duty System, which is assumed for the fuel cell used in this study [77].
Both studies and commercial producers demonstrate that PEM fuel cells have fast dynamics that can allow quick response and ramping times. A study concluded that it is reasonable to assume a 0.2-1.2 response time followed by a power ramp rate of at least 20-30%/second [56]. That would in extension mean that just as for the electrolyzer and battery, dynamics connected to starting and stopping the fuel cell can be disregarded due to the lower resolution of the model. A fuel cell's efficiency tends to vary in relation to the power output [79, 81]. To account for this relation, a 6th-order polynomial ($p(x) = 7{:}1856x^5 - 23{:}936x^4 + 30{:}474x^3 - 18{:}514x^2 + 5{:}2895x - 0{:}0305$) was fitted to resemble such a curve, as shown in Figure 2.7, in order to achieve similar fuel cell efficiency behaviors in the model. To account for the power consumption of connected auxiliaries, the curve has been adjusted by subtracting 0.05 from a_0, thus a 5% reduction of efficiency is assumed.

Figure 2.7: Constructing a 6th order polynomial to resemble a typical fuel cell efficiency curve.

The efficiency decrease of the fuel cell power is assumed to be linear as a function of time. A study found that, given that the relative humidity (RH) can be maintained at high levels of around 70%, a cell voltage degradation of around $2 \mu V/h$ can be assumed [63]. Comparing this value to what was found for electrolyzers, $2 \mu V/h$ corresponds to around 0.0002-0.00075 % per hour of operation. Another study saw a 0.001 %/h degradation over 5100 hours with fuel consisting of 1% methanol [80]. It was also concluded that methanol overall caused a degradation approximately 10 times higher than hydrogen. Thus, several studies point to the fact that the efficiency degradation of fuel cells should be of the same order of magnitude as for electrolyzers. An efficiency degradation of 0.0003 %/h is assumed.

A study by Lipman et.al. (2004) was used as a reference to attain the economic parameters of the fuel cell [81]. Three di erent cost scenarios (low, medium and high) are assumed in the study. The investment costs are assumed as 376, 658 and 940 ¿/kW $_{el}$ (1$=0.94¿). These costs can be con rmed by other studies [83]. The corresponding O&M costs are 19, 49 and 90 ¿/kW $_{el}$-year, given in percentages in Table 2.4. Maintenance of a fuel cell will in addition to ordinary check-ups also include occasional replacement of ine cient and degraded cells.

Table 2.4: Fuel cell parameters used in this study.

Parameter	Value	Unit	Reference
Minimal H_2 consumption	10	% of maximum	[71, 72]
Nominal H_2 consumption	17.76	kg$_{H_2}$/h	[71, 72]
Operational lifetime	20,000	hours	[77]
E ciency decrease	0.0003	%/h$_{operation}$	[63, 80]
Investment cost	376	¿/kW $_{el}$	[81, 83]
Annual O&M cost	5	% of total inv.	[81]

2.6 Hydrogen storage

When considering the use of fuel cells and electrolyzers, the total electricity-to-electricity e ciency is an important parameter to consider. The e ciency when going from electricity to hydrogen and back again is typically around 33% using PEM cells, which is illustrated by Equation 2.7 [11]. This means that it is ine cient and illogical to use electrolyzers and fuel cells as a means to store energy over shorter periods of time, where batteries perform better. But for long-term energy storage, hydrogen can be of greater use as there won't be an energy decrease over time on the same scale as a battery would experience [48, 84].

$$_{total} = _{electrolyzer} + _{storing,\ in} + _{storage\ period} + _{storing,\ out} + _{fuel\ cell} \quad (2.7)$$

Three typical groups of hydrogen storage technologies are physical (e.g compressed gas or cryogenic liquid), adsorption (e.g. in porous materials), and chemical (e.g. in metal hydrides) storage [84, 85]. When deciding what type of storage that should be used, an important parameter is the storage period. In the energy system considered in this study, an electrolyzer is producing hydrogen that is later used in a fuel cell or ammonia/methanol production plant, while also having the option to sell the hydrogen directly to the market. Thus, the hydrogen storage size will most likely be optimized in accordance with the time periods where there is a lack of wind, at least when maximizing pro ts is on the agenda. If reasonable from a design and cost perspective, hydrogen storage may for example be sized to cover one week of low or no wind, while other cases might require storage of larger amounts to cover two or three weeks.

Of the technologies mentioned above, stationary tank storage (for compressed hydrogen) will be considered in this study. This type of storage is a mature storage technology with fast dynamics to enable flexible operation of the energy system while also being relatively cost-effective [84, 85]. There are four different types of stationary tanks, often referred to as Type I to IV, illustrated in Figure 2.8 [85]. Type I is the cheapest option as they are mainly metallic and can typically handle pressures up to 30 bar. For higher pressures, the walls usually need to be quite thick resulting in a significant weight increase. Type II tanks are wrapped in some variation of composite resin, resulting in the tank being lighter and able to handle higher pressures, but at a higher expense. Type III tanks are strong and lightweight as they are completely made out of composite materials, but are wrapped with a metallic lining for extra strength. These tanks can handle pressures around 300-400 bar and in specific cases even 700 bar. Type IV tanks are similar to III tanks in the sense that they are completely made out of composite materials. But instead of a metallic liner, type IV tanks most often use a polymeric liner to increase strength.

Figure 2.8: Four types of hydrogen storage tanks, type I to type IV from left to right.

The main advantage of glass fibre is that it is less expensive. Another minor advantage that could be mentioned is that glass fibre cylinders are more reproof than carbon fibre cylinders. But in terms of weight, the carbon fibre cylinders are advantageous. To achieve the same strength (in terms of pressure), the glass fibre winding needs to be 3 times thicker than the carbon fibre winding. This leads to both higher weights and higher cylinder diameters.

2.6.1 Storage characteristics

A commercial reference from UMOE Advanced Composite, in particular their largest product called "40' ISO high cube" container, is used for initial assumptions [87]. They offer a container with 22 type IV pressure vessels in fibreglass and epoxy resin, holding a total volume of 42.35 m^3 at 450 bar. An average temperature of 8 °C was seen during the period of 1991-2010 in southern Sweden and is assumed as the ambient temperature for the stationary tank in this study [88]. This converts to a tank mass capacity of around 1634 kg using the ideal gas law. However, a more realistic value of the total mass stored would be closer to 1,256 kg, which is assumed in this study [89].

When operating a type III and IV composite tank, lower pressures should be avoided to minimize liner degradation [90, 91]. At low pressures, the liner can start to shrink, crack and nally separate from the laminate. Studies have found that a minimum pressure of around 25 to 30 bar should be maintained to avoid degradation. For that reason, the minimum pressure is assumed to be 30 bar [90]. Studies indicate that composite type IV tanks can be fueled well within one hour, demonstrating dynamics that can be needed in a future energy system [92]. This results in the model not being able to capture tank dynamics within the hourly time resolution. Thus, the mass ow rate is left unconstrained in this study. Auxiliaries' power consumption connected to the storage is neglected, as this is shown to be a small percentage of the total available energy [93].

Figure 2.9: UMOE Advanced Composite's type IV hydrogen storage.

Several studies found an investment cost of 455 €/kg$_{H_2}$ to be reasonable for composite tanks [93, 94, 95]. An annual O&M cost of 2% of the investment [95] and an operational lifetime of 15 years is assumed [96, 97].

Table 2.5: Stationary storage tank parameters (Type IV, composite breglass, 1 container) used in this study.

Parameter	Value	Unit	Reference
Ambient temperature	8	°C	[88]
Volume	42.35	m^3	[87]
Minimum pressure	30	bar	[90, 91]
Maximum pressure	450	bar	[87]
H_2 weight at max pressure	1,256	kg$_{H_2}$	[89]
Maximum mass ow rate	Unconstrained	kg$_{H_2}$/h	[92]
Operational lifetime	15	years	[96, 97]
Investment cost	455	€/kg$_{H_2}$	[93, 94, 95]
Annual O&M cost	2	% of total inv.	[95]

2.7 Ammonia synthesis

Ammonia (NH_3) has a wide range of end-use services, primarily being an important ingredient in for example fertilizer [98]. Around 70% of the NH_3 produced in the world is used to make mineral nitrogen fertilizers, making a signi cant part of the food industry rely on NH_3 production. NH_3 also has a wide range of industrial applications for plastics and synthetic bres etc. For the production of NH_3 the so-called Haber-Bosch (HB) process is assumed to be utilised due to its maturity and widespread commercial use compared to alternative methods [99]. In the HB process, high-purity hydrogen and nitrogen (>99.99%) are passed over a catalyst bed combined with a recycling loop resulting in an overall conversion rate of 97% of the hydrogen. The reaction is illustrated in Equation 2.8, and is most e cient when the process requirements of 400-550 °C and 100-250 bar are sustained.

$$\frac{1}{2}N_2 + \frac{3}{2}H_2 \rightarrow NH_3 \tag{2.8}$$

In HB, the catalyst takes a lot of damage when the production is stopped [100]. If there's no demand for ammonia or even a shortage of reactants, the plant has to be kept in hot standby mode to prevent irreversible damage to the catalyst. The Danish Energy Agency (DEA) indicates that the production rate can be ramped up and down within 30-100% of the maximum production rate [100]. However, unless hot standby mode is utilized, starting the process from ambient conditions can require up to one day to reach full production capacity. Studies suggest that hot standby mode can reduce the start-up time to around 1-3 hours [100, 106]. To avoid catalyst damage and e ciency losses it is therefore preferred to operate the HB loop at a constant load. This results in trade-o s between e ciency and operational exibility [99]. As a result, it is a good idea to operate the HB process at a constant load continuously for the plant's lifetime. This dictates the use of energy storage to power the synthesis loop when there is insu cient renewable power [99].

A key ingredient for NH_3 is nitrogen gas, which is abundantly available in the air. In fact, 78% of air consists of nitrogen, making it more accessible than for example carbon dioxide [101]. Two well-known industrial methods to attain a high-purity stream of nitrogen are cryogenic air separation and pressure swing adsorption [99]. This study will only consider a cryogenic air separation unit (ASU) because this technology is the most mature while also achieving a higher purity of nitrogen. Similar to the Haber-Bosch process, an ASU has very slow dynamics in the order of hours, a ecting the overall exibility of the NH_3 synthesis [102, 103].

2.7.1 Synthesis characteristics

Several studies suggest a power consumption of around 10-12 kWh/kg_{NH_3} for NH_3 synthesis with the HB process, including the production of hydrogen [107, 108]. The hydrogen production can, however, be accounted for by using Equation 2.9 (with mol_{H_2} per mol_{NH_3} shown in Equation 2.8) to transform the power consumption of H_2 to the corresponding amount of NH_3, which is 9.3 kWh/kg_{NH_3}.

$$52{:}3\frac{kWh}{kg_{H_2}} \quad 2{:}016\frac{kg_{H_2}}{kmol_{H_2}} \quad \frac{3}{2}\frac{mol_{H_2}}{mol_{NH_3}} \quad \frac{1}{17{:}031}\frac{kmol_{NH_3}}{kg_{NH_3}} = 9{:}3\frac{kWh}{kg_{NH_3}} \tag{2.9}$$

This value, combined with other studies claiming a power consumption of 0.5-2 kWh/kg_{NH_3} for the synthesis process alone, provides su cient support to assume a similar value [109, 110]. In this study a power consumption of 1 kWh/kg_{NH_3} is assumed for the ammonia synthesis. The ASU process has similar production requirements as HB, hence, the N_2 production is assumed to occur simultaneously and with the same dynamics as the NH_3 synthesis. Studies show that an ASU process tends to consume approximately 0.37 kWh/kg_{N_2}, which is assumed in this study [104, 105]. Additionally, a minimum production rate of 30%, and 1%/min ramp time is assumed. Standby will not be allowed in this study, as the DEA describes a signi cant increase in investment costs to enable such high operational exibility [100].

A study suggests an investment cost of around 144 M¿, corresponding to a production of 123,400 t_{NH_3}/year, including the capturing of N_2 [111]. As the study assumes 7500 hours of operation per year, the investment in relation to the production rate is 8,775¿/(kg $_{NH_3}$/h). Note that 123,400 t_{NH_3}/year at 7500 hours/year corresponds to an hourly production of around 16,500 kg_{NH_3}/h. As investments in large chemical plants tend to be cheaper for larger production volumes, this investment cost is seen as reasonable as long as production volumes are kept at similar magnitudes. The same study also assumes an O&M cost of 1.5% of the initial investment cost and a market price in the range of 350-850 ¿/t $_{NH_3}$. Another study claims that the price of NH_3 was 450¿/t $_{NH_3}$ in December 2020, and went up to 1,500 ¿/t $_{NH_3}$ by December 2021 [109]. Hence, the market price is a parameter that should be further evaluated when modelling. Finally, the study assumes a catalytic bed replacement cost of 30% of the initial investment, after 10 years, which is assumed in this study.

Table 2.6: Ammonia synthesis parameters used in this study.

Parameter	Value	Unit	Reference
Power consumption N_2 prod.	370	kWh/ton_{N_2}	[104, 105]
Power consumption NH_3 prod.	1000	kWh/ton_{NH_3}	[107, 108, 109, 110]
NH_3 minimum production rate	30	%	[100]
NH_3 production ramping	1	%/min	[100]
NH_3 standby	Not allowed	-	[100]
Investment cost	8,775	¿/(kg $_{NH_3}$/h)	[111]
Stack replacement frequency	10	years	[111]
Replacement cost	30	% of total inv.	[111]
Annual O&M cost	1.5	% of total inv.	[111]
NH_3 market price	450-1,500	¿/ton	[111, 109]

Since the HB process requires conditions to stay around 400-550 °C and 100-250 bar, heat integration with the rest of the energy system can minimize costs and electricity demands [99]. Though, to further simplify the energy system this study will neglect heat integration of the HB process. This study also assumes that overconsumption of reactants in the synthesis is included in the power consumption, and can therefore be neglected as well. Finally, the suitability of nitrogen storage will not be evaluated as it is assumed that the produced NH_3 can be sold directly to the e-fuel market. A more realistic way to sell e-fuels would be via a cargo ship or pipeline, but these costs are neglected as fluctuations of the NH_3 market price will be evaluated instead. This way, a higher price could hypothetically correspond to a cheaper market price but with docking or pipeline investments included.

2.8 Methanol synthesis and carbon capture

Methanol (MeOH) is a versatile chemical compound that is often used as a starting point for producing a wide range of other substances. A clear advantage when producing MeOH from hydrogen is that MeOH is in a liquid state at ambient conditions, making transport and storage less complex than for example H_2 [112]. MeOH can also be blended into different grades of gasoline to be used in existing combustion engines, which in extension can reduce CO_2 emissions given that the MeOH is renewable [113]. In this study the renewable aspect is central, and thus it is important to ensure that the entire procedure including the synthesis and use of MeOH is kept carbon neutral.

MeOH production consists of three main steps; H_2 production, CO_2 capture and MeOH synthesis. Hydrogen is, as illustrated in Figure 1.1, produced from electrolysis with renewable electricity from the wind farm.

Commercially, CO_2 can be captured from industrial flue gas streams with typically high CO_2 concentrations, such as industrial furnaces and cement plants [114]. A typically well-known and mature method to capture CO_2 in such streams is through chemical absorption with an amine-based sorbent [116]. With recent developments in the area of carbon capture, a fairly recent technology called Direct Air Capture (DAC) can also be used to capture CO_2 directly from the surrounding air [115]. Given that the unit is powered by renewable electricity and that the CO_2 is stored for an extended period of time (e.g. in plastic cable or underground), this carbon capturing can result in negative emissions. However promising, DAC still needs further developments to reduce costs and resource intensity to compete with other capture technologies like chemical absorption.

MeOH can be synthesized in several ways, but given an energy system where the reactants are produced with renewable electricity, CO_2 hydrogenation is a suitable option [117]. The hydrogenation process can be described as a chemical equilibrium between three main reactions, given in Equation 2.10, where the desired end-product can be enhanced by adjusting the reaction conditions and by using a suitable catalyst.

$$\begin{aligned} CO + 2H_2 &\rightleftharpoons CH_3OH \\ CO_2 + H_2 &\rightleftharpoons CO + H_2O \\ CO_2 + 3H_2 &\rightleftharpoons CH_3OH + H_2O \end{aligned} \tag{2.10}$$

According to a study, a feed ratio of H_2/CO_2=3 at 250°C and 5MPa should result in an outgoing flow of 27% CO_2 and 68% CH_3OH [117]. Membranes can also be used to further increase the MeOH yield by selectively removing reaction products from the system, common ones being zeolite and palladium-silver membranes [112, 117]. The main processes requiring energy in the MeOH synthesis, with CO_2 capture and H_2 electrolysis excluded, are the compression (of reactants) and distillation (of products) [118]. A study by Tidona et. al. (2013) suggests that the efficiency of the synthesis can be reduced by adjusting the pressure at which the reactants are recycled.
The compression of reactants and synthetization of MeOH will produce thermal heat as a bi-product, which theoretically could be heat integrated with the rest of the energy system to improve the overall efficiency. This would by extension improve the energy efficiency of the process.

2.8.1 Synthesis characteristics

Similarly to the HB process, CO_2 hydrogenation requires the temperature and pressure to be maintained, hence resulting in an inflexible process requiring energy storage systems for a consistent electricity supply [100]. Some flexibility can be attained when choosing MeOH production from electricity instead of the traditional production method using natural gas. However, as the synthesis stage still needs conditions of at least 250°C and 5MPa to be maintained to avoid catalyst decomposition, stopping the production due to a temporarily high electricity price is rarely an option. The minimum production rate is supposedly 40%, a number that over the coming years can be reduced to 10% according to the DEA. This could be a result of recent interest in higher operational flexibility, as combing methanol production with wind farm production is a hot topic today. Nevertheless, a 40% minimum rate is assumed in this study. Finally, the DEA states that cold start-ups should be avoided, but that the process can maintain a hot standby mode for several days, enabling start-up times faster than 3 hours. Hence, standby is allowed in this study, along with a ramp-up of 1%/min to result in a 2-hour start-up [100].
For the capturing of CO_2, an industrial flue gas stream of high CO_2 concentration is assumed to be available nearby the site, as shown in Figure 1.1, without any limitations considering mass flow dynamics. The CO_2 is also assumed to be captured with chemical absorption using an amine-based sorbent due to its frequent commercial use. [116].

Studies suggest that the power consumption of MeOH synthesis from CO_2 hydrogenation should be in the range of 0.3-1.3 kWh/kg_{MeOH} [119]. A specific value averaged from the result of three studies was calculated to 0.72 kWh/kg_{MeOH}, which is assumed in this study [119, 120, 121]. In addition, the power consumption of chemical absorption was found to be around 0.29 kWh/kg_{CO_2} according to several studies [122, 123, 124].

The investment cost of a methanol production process seems to vary a lot, perhaps due to the many possible variations of the process and what different studies chose to include. For simplicity, investment costs were transformed to the unit €/(kg $_{MeOH}$ /h), implying a specific cost per production capacity per hour. The reason why that unit is used, instead of €/kW, is that the wattage can significantly vary between studies, as the synthesis consumes both heat and electricity. One study found a specific investment cost of 806 €/(kg $_{MeOH}$ /h) including a CO_2 capture system [125]. A second study found the same parameter to be 7,100 €/(kg $_{MeOH}$ /h) [135], while a third saw it could go as high as 22,000 €/(kg $_{MeOH}$ /h) which demonstrates the large variations [136]. Thanks to some commercial references given by Euromekanik, it was implied that a cost of 7,100 €/(kg $_{MeOH}$ /h) should be closest to reality. The chemical absorption system is assumed to be included due to its, relatively, low cost [130].

The catalyst is assumed to need replacement every 5 years, with a cost at 20% of the total investment [127, 128]. The annual O&M cost is assumed to be 12% of the initial investment cost [135]. The MeOH market price is assumed to range between 400 and 800 €/ton $_{MeOH}$, in order to consider different future scenarios [136].

Table 2.7: Methanol synthesis parameters used in this study.

Parameter	Value	Unit	Reference
Power consumption CO_2 capture	290	kWh/ton_{CO_2}	[122, 123, 124]
Power consumption MeOH prod.	720	kWh/ton_{MeOH}	[119, 120, 121]
MeOH minimum production rate	40	%	[100]
MeOH ramping	1	%/min	[100]
MeOH standby	Allowed	-	[100]
Investment cost	7,100	€/(kg $_{MeOH}$ /h)	[125]
Stack replacement frequency	5	years	[127, 128]
Replacement cost	20	% of total inv.	[127]
Annual O&M cost	4	% of total inv.	[125]
MeOH market price	400-800	€/ton $_{MeOH}$	[136]

The simplifications used for the ammonia synthesis, given in the last paragraph of Section 2.7.1, will apply to the methanol process as well. Accordingly, this study neglects the potential of heat integration as well as intermediate methanol storage. Furthermore, the overconsumption of reactants is assumed to be included in the power consumption.

2.9 Energy system economics

This study will evaluate the techno-economical feasibility of a system consisting of a wind farm coupled with an electrolyzer, batteries etc. Depending on the case, there are a lot of important economical parameters that investing companies and societal decision-makers may want to consider. It can involve parameters such as expected incomes from hydrogen and electricity sales, net present values and rate of returns. This section will describe the parameters that are used to present key results in this study, and some key assumptions are summarized in Table 2.8.

Table 2.8: Economical parameters used in this study.

Parameter	Value	Unit	Reference
USD to EUR	0.94	EUR/USD	Assumption (Feb, 2023)
GBP to EUR	1.14	EUR/GBP	Assumption (Feb, 2023)
SEK to EUR	0.09	EUR/SEK	Assumption (Feb, 2023)
Discount rate	4.5	%	[131]
Energy system lifetime	20	years	Assumption

Firstly, all economic values are given in¿ (EUR). For parameters found in studies using either¿ or $, a conversion rate of 1.14¿/¿ and 0.94¿/$ was assumed respectively. For SEK, a rate of 0.09¿/SEK was assumed.
The technical lifetime of the energy system is assumed to be 20 years, as this was a recommended value in the utilized software. A discount rate of 4.5 % was suggested to be ideal for a scienti c study such as this one and is therefore assumed [131].
One important technical parameter seen frequently in the results is the amount of electricity supplied to the grid. Depending on what electricity price is used, the amount of electricity supplied can have a signi cant impact on the nal results. As the system can inject electricity, while also supplying hydrogen, these incomes will most often be referred to as Electricity income and Hydrogen income, given in¿M
For all di erent system con gurations, the utilized software will calculate costs such as investment costs, operational costs and total incomes. From all di erent incomes and expenditures, a nalized net present value (pro t) and payback time (PBT) can also be calculated. These two parameters are used to compare di erent cases from an economic feasibility standpoint. It should, however, be noted that some scenarios can be compared based on a negative pro t, while their PBT seems to be the same, as the software will end the simulation after 20 years.
Important notice: As it was not possible to scrutinize the equations and algorithms of the software's calculation code, and also since input assumptions and data come with some uncertainties, it is important to avoid focusing on individual result values, but instead on the displayed trends and behaviors in the system.

3
Method

3.1 The system under study

In the energy system frequently referred to, wind power is used to power an electrolyzer while also having the option to supply electricity either to the grid, a nearby industry, an electrolyzer or a battery. Apart from electricity, there is also important decision-making connected to hydrogen produced from electrolysis. Hydrogen can either be sold, stored in containers for later use in a fuel cell to cover peak loads in the power grid, or used to produce a more complex e-fuel such as ammonia or methanol. Given that the facility is managed by a pro t-making company this decision strategy usually comes down to maximizing pro ts from selling these e-fuels. Still, other ambitions such as supplying a certain grid- or e-fuel demand could also come into play. Limitations in the production processes are also expected to play a large role in the energy system, due to the low operational exibility. In certain systems ramping down a process might be more pro table than investing in larger energy storages.

3.2 Study framework

The work of this study began with a literature review and data collection phase, to establish a base level of understanding for the studied energy system. Values assumed for the di erent units utilized in the system had to be veri ed either by scienti c studies, or commercial references, as given in Table 2.1, 2.2, 2.3, 2.4, 2.5, 2.6 and 2.7. Yet, some parameters are left unconstrained, for example, the number of batteries and hydrogen containers, as such values can be case-speci cally optimized. In Section 2, simpli cations such as neglecting heat integration of certain units and resolution limitations are explained. These simpli cations are further discussed in Section 5.2.2 and 5.1.1 respectively.
In Section 2, the trend of using VMSs is described, justifying its importance if the share of RES should increase. Since the use of peak shifting (with batteries) and peak absorbing (with electrolyzers) is evaluated in this study, the relevance of VMSs is in extension assessed as well. However, the agenda of supporting the grid compared to maximizing pro ts a ects the results to a great extent.
When all unit data was collected, the energy system could be con gured and adjusted. Some values had to be reconsidered, along with certain data pro les that simply delivered inconsistent results. Resulting graphs and tables were compiled in the Appendix to present the full picture of depicted behaviors.

The most important takeaways are brie y explained in results and outlined in tables and graphs. Assumptions that signi cantly impact the results are further explained in Discussion, Section 5, along with societal, ethical and ecological aspects, before key conclusions of the study are presented.

3.3 Model framework

The energy system was constructed using the software Odyssey from Seed Energy, which is designed for modelling complex energy systems to assess technical, economical and environmental indicators. Odyssey displays the system architecture as shown in Figure 3.1.

Figure 3.1: System architecture in Odyssey.

Running the model will produce graphs displaying how calculated parameters are changing over a year. The software will also calculate total values for wind power potential, injected electricity, sales income etc. The operational lifetime of the entire system can be set to several years, and the initial value recommended by Odyssey is 20 years. Hence, Odyssey is able to accurately calculate not only technical behaviors such as long-term degradation but also economic parameters like pay-back time and lifetime pro ts. Models can also be optimized by the software according to both economical and technical parameters, and this ability allows for several scenarios to be compared and evaluated. Using energy balances with several user-de ned parameters, the model can also realistically calculate the produced mass of hydrogen, nitrogen, and ammonia for every time step.

3.3.1 Controllers

In Odyssey, the decision-making connected to unit operations is dictated by a set of so-called controllers. There are usually two controllers for every bus in the architecture (the vertical line connecting all units), see Figure 3.1, along with specific unit controllers. For every controller, there are algorithms to choose from and values that can be used to adjust these algorithms. The controllers that are relevant to this study, are listed below:

- Positive electrical balance
- Negative electrical balance
- Electrolyzer system - Start/Stop & Production constraint
- NH_3 synthesis - Start/Stop & Production constraint
- MeOH synthesis - Start/Stop & Production constraint

The positive and negative electrical balance controllers can be configured with a pre-defined order of utilization between electrolyzer, battery and grid injection (positive balance) and fuel cell, battery and grid extraction (negative balance) depending on if the system experiences a surplus or deficit of electricity. This surplus/deficit is calculated from what is left after the produced wind power has been supplied to the electrical load (if a load has been defined). There are also a set of algorithms that can be used instead of a pre-defined order, e.g. "Algorithm 5", which is described in Table 3.1. Such algorithms are defined by Odyssey, and depending on the case and objective a specific algorithm can provide options connected to energy system operations that a defined order wouldn't consider. Nevertheless, pre-defined orders were used predominantly in this study to remain focused on the key evaluations given in Section 1.1.

Table 3.1: Controller algorithms used in this study.

Positive electrical balance		
Pre-defined order	The user defines the order of utilization during a surplus of electricity.	- Battery - Electrolyzer - Grid injection
Algorithm 5	Adjusts the electrolyzer to absorb the surplus (with electrolyzer dynamics applied). If there is no remaining surplus, batteries discharge to the electrolyser. Otherwise, batteries charge.	
Negative electrical balance		
Pre-defined order	The user defines the order of utilization during a deficit of electricity.	- Battery - Fuel cell - Grid extraction

The electrolyzer can be controlled by a start/stop constraint as well as a production constraint. These are especially relevant when addressing speci c situations and certain technical behaviors that in general won't be covered in this study. A speci c situation could be to operate according to electricity price thresholds, adjusting units to high and low prices. Hence, the electrolyzer controllers are neglected. Throughout this study, the H_2 production is adjusted according to power availability, by using a pre-de ned order as shown in Table 3.1, making additional start/stop and minimum production constraints redundant.
The NH_3 and MeOH processes are handled similarly in this study and are primarily distinguished from each other by their di erent power consumptions, dynamics and investment costs. From a controller perspective, they will both be controlled by a production constraint algorithm that adjusts the e-fuel production rate according to the H_2 and NH_3 or MeOH storages' SoC. The algorithm constructs a scaling factor, SF, which is calculated from the SoCs, as shown in Equation 3.1 for the MeOH synthesis, and can be tuned by two user-de ned exponents illustrated in Figure 3.2.

$$SF_{MeOH} = (1 \quad SoC_{MeOH}^{Exp_{MeOH}}) \; SoC_{H_2}^{Exp_{H_2}} \tag{3.1}$$

Figure 3.2: Scale factor depending on the hydrogen and methanol storage SoC (Exp_{MeOH} = 0.5 and Exp_{H_2} = 2).

In this study, Exp_{H_2} is set to 1, while Exp_{MeOH} is set to 0 since methanol intermediate storage is neglected. Using this method to constrain the amount of NH_3 or MeOH produced, depending on the hydrogen storage SoC, will result in a more exible Odyssey model. However, optimizing the energy system according to certain parameters, such as pro t or grid injections, can be even more complex due to the added dependencies between electrolysis, e-fuel production and hydrogen storage.

3.3.2 Cases

Four cases constitute the main results and evaluations of this study. Specifically, a "grid support" case together with one case for each of the three mentioned e-fuels, as shown by the figures in Appendix A. The initial "grid support case" was assumed in order to establish and evaluate specific model behaviors connected to for example electricity prices and transformer limitations. For example, the electricity prices of 2019 and 2022 were compared to establish whether they were reasonable, and also if there could be any sources of error. Different transformer capacities were also compared for the same reasons. Finally, the relevance of batteries and hydrogen in a grid support case was established. The hydrogen case is expected to have the highest operational flexibility due to the electrolyzer's ability to standby and quickly ramp up or down its production rate. The economic performance of this case compared to the grid support case will likely be significantly impacted by the hydrogen market price. The ammonia and methanol cases will combine the flexibility of the electrolyzer with a hydrogen storage to enable a continuous and efficient e-fuel synthesis avoiding any catalyst damage. The synthesis dynamics, depicted in Table 2.6 and 2.7, will be taken into consideration and probably lead to one being more advantageous than the other. Recommendations are given both from a technical and economical standpoint.

4

Results

4.1 Electrolyzer standby

During modelling, a particular behavior in the electrolyzer operation had to be addressed before cases could be evaluated. It was seen that when wind power production dropped below 3.6 MW a surplus of electricity arose that subsequently was injected into the grid. This was because electrolyzer standby mode was allowed, stopping the electrolyzer altogether when the available power dropped below the amount required to keep one unit running, as indicated in Section 2.5.1. This gave rise to a surplus of electricity instead as shown in Figure 4.1. From a hydrogen case standpoint, where hydrogen production is first priority, it is noteworthy that grid injections occur (lower graph in red) at periods when the electrolyzer isn't running (upper graph in green) while the wind farm is producing (upper graph in red). Further explained, this means that the energy system is selling electricity instead of using it in the electrolyzer, even though the case objective is to prioritize hydrogen production. To easier illustrate this behavior, the minimum production rate of the electrolyzer was temporarily set to 1,300 kg_{H_2}/h, as 65 kg_{H_2}/h is close to zero in relation to the other values in the system.

Figure 4.1: Production and consumption during one year. Allowing electrolyzer standby, minimum production rate = 1,300 kg_{H_2}/h, no battery. Blue ovals mark the time periods when electrolyzers are on standby. (Upper graph in red: wind farm production, green: electrolyzer. Lower graph in red: grid injection.)

In Appendix B, resulting graphs from di erent combinations of electrolyzer standby, minimum electrolyzer production rates and additional batteries were compared. It can for example be seen in Figure B.2 and B.3 that suppressing standby mode will have a similar e ect on grid injections (lower graph in red) as allowing standby and adjusting the minimum production to 0 kg_{H_2}/h, which is to remove most injections. Further, it can also be seen in Figure B.2 that by suppressing electrolyzer standby, electricity has to be extracted from the grid in order to keep the electrolyzer running at its minimum rate. Figure B.3 illustrates that allowing standby and an electrolysis process in the complete range of 0-4,555 kg_{H_2}/h, though unrealistic, will result in a smooth utilization of the wind production.

Figure B.4, B.5 and B.6 display the e ect of adding enough batteries to completely cover these surpluses and de cits. It can be seen that both grid injections and extractions at most points are removed or at least reduced. Comparing Figure B.2 and B.5 shows that a battery can replace the need for grid extractions, which is further discussed later in the results.

Considering the electrolyzer's characteristics, it can be di cult to determine which case should be utilized in this study. The hourly resolution of the data makes some unit dynamics redundant, as they can't be realised by the model anyway. Going below an electrolyzer's minimum production rate for more than an hour should call for electrolyzer standby to be allowed. Alternatively, grid extractions can be used to cover the de cit.

In a realistic setting, an electrolyzer's key advantage is its cold-start capability allowing the unit to start and stop exibly. This is why electrolyzer standby, unlike ammonia and methanol synthesis, shouldn't be avoided. In a system such as the one considered in this study, a production rate range of 65-4,555 kg_{H_2}/h can also be seen as low and exible enough to avoid such "unnecessary" grid injections. In this study, electrolyzer standby and a minimum production rate of 65 kg_{H_2}/h is used.

4.2 Grid support case

4.2.1 Electricity price

A key gure to compare with the e-fuel cases is the total pro t if the wind farm had been operated in a traditional fashion, which is to sell all electricity produced directly to the grid. By neglecting the addition of electrolyzers, batteries, fuel cells etc., the e ect of di erent electricity prices on a traditional system's economic performance can be compared. The total incomes, pro ts and PBTs were calculated, and have been compiled in Table 4.1.

Table 4.1: Electricity sales income, pro t and payback time (PBT) for di erent electricity prices.

Electricity price	El. income [M¿]	Pro t [M ¿]	PBT [years]
SE4 2019	2,406	-1,028	>20
SE4 2022	9,298	5,864	4
50 ¿/MWh	4,357	923	14
100 ¿/MWh	8,714	5,280	6

As the PBT of a wind farm should be in the range of 4-7 years, the electricity price in SE4 during 2022 is seen as most appropriate to attain realistic results from the model. Using a constant price of 100 ¿/MWh could also be reasonable, but as a 4-year payback period was achieved without any transformer limitations, it is expected that this number will increase with a decreasing transfer capacity and electricity sales income. In the following cases, the two SE4 prices will be used to nuance the results and in extension recommendations given based on future developments.

4.2.2 Transfer capacity

As shown in Figure 2.2, there are di erent transfer capacities that can be considered in an energy system such as the one studied. A possible assumption, though perhaps unrealistic, is that a wind farm can supply unlimited amounts of electricity to the power grid. The assumed transfer capacity can also be reduced by taking limitations connected to transformers and transmission lines into account, as explained in Section 2.3. There are also cases, when the power grid's ability to receive electricity is limited, at which point the capacity can experience similar variations as an electricity zone's grid demand.
The alternatives mentioned above, all of which are illustrated in Figure 2.2, have been compiled in Table 4.2 along with resulting key parameters. When comparing these grid transfer capacities, the SE4 2022 electricity price was used. The di erent capacities are also displayed in Figure C.1, C.2, C.3 and C.4. From them, it is illustrated how the capacities a ect the total wind power utilized (upper graph in red) compared to what is available (upper graph in blue), in the gures referred to as wind farm production potential. The lower graphs in all of the gures show the transfer capacity being used.

Table 4.2: Electricity supplied, pro t and PBT for di erent transfer capacities.

Transfer capacity	El. supplied [GWh]	Pro t [M ¿]	PBT [years]
Unlimited	4,555	5,864	4
Actual SE4	4,555	5,864	4
SE4 - 1 GW_{peak}	3,851	4,492	5
500 $MW_{constant}$	3,433	3,573	6
SE4 - 500 MW_{peak}	2,361	1,382	11

From Table 4.2, the connection between transfer capacity and the amount of electricity supplied to the grid is clear, higher capacity equals more electricity injected.

With more electricity injected, the pro ts will also increase, along with a shorter PBT. When considering the case of a large-scale o shore wind farm, it is reasonable to assume that the owner wants to maximize the electricity injected, in order to minimize the PBT. A simple observation to make is that investments towards a 1 GW wind farm will be less pro table if most of the electricity produced will have to be curtailed due to signi cant limitations in transfer capacity. Based on previous studies, all the resulting PBTs of the di erent capacities are seen as reasonable [26, 27, 28, 29]. Thus, all capacities can be used in this study when other behaviors are evaluated.

4.2.3 Peak-load shifting scenario

When evaluating the energy system's ability to manage variations and supply more electricity with batteries or fuel cells than previously possible, the parameters used in Table 4.2 were assessed. The model was con gured as shown in Table 4.3, with di erent options for the rst priority unit in the positive and negative electrical balances, depending on the case, along with di erent transfer capacities. Unlimited grid transfer was however neglected in the evaluations since there is no need for peak-load shifting when all electricity can be injected instantly.

Table 4.3: Grid support case: peak-load shifting con guration.

Parameter	Value
	Controllers
Positive electrical balance	1. Battery / Electrolyzer.
	2. Grid injection.
Negative electrical balance	1. Battery / Fuel cell.
	2. Grid extraction
	Power grid
Electricity price	SE4 2022
Grid transfer	1 GW_{peak} / 500 $MW_{constant}$ / 500 MW_{peak}

4.2.3.1 Batteries

The option of adding batteries was evaluated in order to establish if they can increase the total pro t of the energy system. As every battery has a capacity of 307 kWh, a relation between pro t and battery capacity could also be calculated. Di erent numbers of batteries were added to establish if an optimized value could be found, all of which were run at various transfer capacities. All results are shown in Appendix C.2 (Table C.1, C.2 and C.3). Outlined below, in Table 4.4, are the numbers of batteries that maximized the pro ts for the di erent transfer capacities.

Table 4.4: Resulting amount of electricity supplied to the grid, investment cost, and payback time (PBT), when maximizing the pro t from the addition of batteries to the grid support case for di erent grid transfer capacities.

	1GW $_{peak}$	500MW $_{constant}$	500MW $_{peak}$
No. of batteries	3,291	2,794	2,156
Energy capacity [MWh]	1,010	858	662
El. supplied [GWh]	2,843	2,822	2,794
Investment [M¿]	3,954	3,526	2,423
Pro t [M ¿]	4,552	3,619	1,405
PBT [years]	5	6	11

Furthermore, along with all resulting key parameters, the relation between pro t and electricity supplied has been plotted against the number of batteries for a 500MW$_{peak}$ capacity in Figure 4.2.

Figure 4.2: Pro t as a function of the supplied electricity (Transfer capacity: 500MW$_{peak}$). Note: 1,000 batteries correspond to 307 MWh.

The same relations for each respective transfer capacity are summarized in Figure C.5, C.6 and C.7 in the Appendix. By approximating the pro t increase as linear between zero batteries and the maximized point, the pro t per storage capacity can be calculated as 34.7, 53.6 and 59.4 ¿/MWh $_{battery}$ for the 500MW$_{peak}$, 500MW$_{constant}$ and 1GW$_{peak}$ limits respectively. Thus, the highest battery pro t was seen at 1 GW$_{peak}$ transfer capacity. It can also be seen across all capacities, that batteries will increase the amount of electricity supplied to the grid. This is excellent from a wind farm owner's perspective, as wind energy curtailment is reduced while pro ts are increased.

4.2.3.2 Hydrogen

The main advantage of using electrolyzers and fuel cells as a means to shift peak-loads is the ability to store hydrogen over longer periods, with reduced energy losses over time than batteries o er. The main disadvantage, however, is the low round-trip e ciency going from electricity to electricity. The pro tability of adding electrolyzers and fuel cells was evaluated, and three main parameters were adjusted to

compare di erent scenarios. These parameters were electrolyzer capacity, fuel cell capacity, and the number of hydrogen containers. A 500MW_{peak} transfer capacity was used, as the same trends were seen across all alternatives.
For every electrolyzer and fuel cell capacity, the number of hydrogen storages could be optimized in order to maximize the pro t. By assuming an electrolyzer and fuel capacity of 250 MW, the results depending on the number of hydrogen containers can be seen in Table C.4. Keep in mind that the maximum capacity per container is 1,256 kg_{H_2}, making the optimized storage for a 1 GW wind farm with a 250 MW electrolyzer and fuel cell approximately 180 $tons_{H_2}$. The relation between the supplied electricity and pro t can subsequently be illustrated in Figure C.4.

Figure 4.3: Pro t as a function of the supplied electricity (Electrolyzer: 250MW. Fuel cell: 250MW. Transfer capacity: 500MW_{peak}). Note: 50 hydrogen containers correspond to 63 $tons_{H_2}$.

By comparing other combinations of electrolyzer, fuel cell and optimized storage capacities, see Table 4.5, it was seen that the highest pro t was attained if no additional investment was made at all. However, peak-load shifting is still seen as technically feasible as the electricity supplied is seen to increase in relation to the unit capacities.

Table 4.5: Resulting amount of electricity supplied to the grid, investment cost, and payback time (PBT), when maximizing the pro t from the addition of fuel cells and electrolyzers to the grid support case (Electricity price: SE4 2022. Transfer capacity: 500MW_{peak}).

Electrolyzer [MW]	50	150	100	150	250
Fuel cell [MW]	50	50	100	150	250
H_2 storage cap. [tons]	10	50	77	103	180
El. supplied [GWh]	2,377	2,401	2,419	2,439	2,478
Investment [M¿]	2,772	2,886	2,869	2,948	3,116
Pro t [M ¿]	1,197	1,102	1,042	862	488
PBT [years]	11	12	12	13	16

Looking at Table 4.5, it can be seen that the fuel cell capacity was either equal to that of the electrolyzer, or lower. This is because of the fuel cells' high hydrogen consumption in relation to the electrolyzers' hydrogen production. Figure C.8 and C.9 illustrate how the hydrogen SoC (upper graph in blue) varies over a 3-month period. The gures show how a 150-50 MW scenario will increase and decrease the storage SoC at similar rates, while the 100-100 MW scenario depletes the storage faster than it is re lled. This could be a reason why the 150-50 MW scenario has a comparable investment cost and amount of electricity supplied, but a higher pro t. Another reason could be the decreased O&M cost of the fuel cell and hydrogen storage, which is signi cantly reduced when going from 100 MW and 77 tons H_2 to a 100 MW and 50 tons H_2 capacity.
Lastly, Figure C.10 shows how a 250 MW electrolyzer combined with a 250 MW fuel cell can utilize almost all of the wind power potential (lower graph, wind power potential in blue and utilized wind power in red), at a transfer capacity of 500 MW_{peak}. This is a signi cant improvement compared to a traditional wind farm with the same transfer capacity, shown in Figure C.4.

4.2.3.3 Investment strategy

Comparing the two methods of peak-load shifting shows that the most economically incentivized technology is batteries. Using hydrogen as a means to store energy was shown to be expensive, and a case where electrolyzers and fuel cells resulted in higher pro ts could not be found. However, the fact that a method doesn't give higher pro ts, doesn't imply that it is a bad idea. By instead comparing the investment costs to the utilized wind energy (UWE), hydrogen could be seen as a competitive choice. The additional UWE per additional investment along with the additional electricity supplied per investment is illustrated in Table 4.6, and shows that hydrogen can be a cost-competitive option. That is, from a wind utilization point.

Table 4.6: Comparison of traditional grid support and pro t-maximized peak-load shifting scenarios, considering utilized wind energy (UWE), amount of electricity supplied to the grid, and investment cost (Electricity price: SE4 2022. Transfer capacity: 500MW_{peak}).

Battery [MWh]	-	662	-	-	-	-	-
Electrolyzer [MW]	-	-	50	150	100	150	250
Fuel cell [MW]	-	-	50	50	100	150	250
Hydrogen storage [ton]	-	-	10	50	77	103	180
UWE [GWh]	2,361	2,427	2,429	2,611	2,678	2,773	2,960
El. supplied [GWh]	2,361	2,423	2,377	2,401	2,419	2,439	2,478
Investment [M¿]	2,700	2,794	2,772	2,886	2,869	2,948	3,116
Add. UWE/inv. [MWh/M ¿]	-	702	944	1344	1876	1661	1440
Add. el. supp./inv. [MWh/M ¿]	-	660	222	215	343	315	281

The most pro table hydrogen solution (from the few combinations modelled in this study) is a 100 MW electrolyzer with a fuel cell of the same capacity and a hydrogen storage capacity of 77 tons, corresponding to 61 hydrogen containers. That still results in a decreasing pro t compared to instant grid injections. Nevertheless, the additional energy that otherwise would have been curtailed from the wind farm, is 317 GWh in total. That corresponds to a curtailment reduction of 1,876 MWh per additional M¿ investment. This scenario would also result in the highest increase of electricity supplied to the grid per additional investment out of all scenarios peak-load shifting with hydrogen. Though, considering the electricity supplied, batteries can result in an increase per investment that is approximately double what hydrogen o ers at 660 additional MWh/M¿. The choice between batteries and hydrogen can then boil down to the question if utilized wind energy is more important than electricity supplied.
Traditionally, electricity supplied should be of higher importance than wind utilization from a wind farm owner's perspective, since grid injection is re ected in the incomes and pro ts. The most economically viable option is therefore still batteries, with its additional 660 MWh / M¿ battery investment and 34.7 k€/MWh increased pro ts. It should be noted that wind utilization and electricity supplied per investment were calculated for the number of hydrogen containers or batteries that were seen to maximize the total pro t. It is reasonable to assume that the maximum pro t scenario should be cost-competitive in other aspects as well, but it should also be possible to nd an optimized scenario to maximize this speci c parameter.
Comparing additional UWE and electricity supplied per additional investment builds an understanding of the energy system as well. The battery scenario with 702 MWh_{UWE}/M¿ and 660 $MWh_{El:supp:}$/M¿ shows that an additional investment will bring an almost equal amount of electricity supplied to the grid as is supplied from the wind farm. That small di erence should be an e ect of losses such as capacity degradation and self-discharge. For the use of hydrogen, however, the electricity-to-electricity e ciency at approximately 33% results in high utilization of wind energy per investment, while a small part of that is re ected in the income. As peak-load shifting with electrolyzers and fuel cells proved cost-ine ective, the addition of fuel cells was not evaluated for the other cases in this study.

4.3 Hydrogen case

From Section 4.2.2, the transfer capacity's e ect on the amount of electricity supplied, pro t and PBT is evaluated. Considering the current case objective of producing hydrogen, the transfer capacity is directly connected to the amount of electricity that can be injected into the grid. An unlimited transfer capacity would give a higher electricity sales income and by extension a higher pro t, compared to a 500MW_{peak} capacity. This straightforward e ect is also seen when evaluating the electrolyzer capacity. Since the electrolyzer acts as a base load with the highest priority in the system, transfer capacity would only a ect the peaks produced that the electrolyzer can't absorb. Comparing di erent electrolyzer capacities shows that an unlimited transfer capacity simply lets the electrolyzer capacity dictate how much of the produced electricity will be sold vs how much is used to produce and sell hydrogen

instead, as illustrated in Figure D.1, D.2 and D.3. Hence, the transfer capacity was initially assumed unlimited.
From Figure D.1, D.2 and D.3, it is also seen how an increased electrolyzer capacity resulted in more hydrogen being produced, while less electricity could be injected to the grid. This resulted in a trade-o between exporting electricity or producing hydrogen, as Figure 4.4 presents.

Figure 4.4: Total amount of hydrogen produced and electricity supplied vs. electrolyzer capacity (Transfer capacity: unlimited).

This trade-o was very much dependent on the electricity and hydrogen market prices. Since the electrolyzer's power consumption starts at 54.9 kWh/kg$_{H_2}$ at the BoL (which goes up to 65.9 kWh/kg$_{H_2}$ during its lifetime) and the market price is in the range of 1.3-5.5¿/kg$_{H_2}$, as given in Table 2.3, the value per energy can be calculated to vary between 21-105¿/MWh. More accurately, the range can be split into 25-105¿/MWh and 21-88 ¿/MWh at electrolyzer BoL and EoL respectively. As the electricity price of 2022 tends to stay above this value, as seen in Figure 2.3, this resulted in electrolyzer investments being unpro table. This can be seen in Figure 4.5 and 4.6. Note that two di erent investment costs were used as well.

Figure 4.5: Pro t from hydrogen production over the total system lifetime, as a function of electrolyzer capacity, for di erent market prices and investment costs. Compared to a traditional grid support case, see Table 4.1, which constitutes a pro t baseline by which the other cases can be compared. (Transfer capacity: unlimited. Electricity price: SE4 2019).

Figure 4.6: Pro t from hydrogen production over the total system lifetime, as a function of electrolyzer capacity, for di erent market prices and investment costs. Compared to a traditional grid support case, see Table 4.1, which constitutes a pro t baseline by which the other cases can be compared. (Transfer capacity: unlimited. Electricity price: SE4 2022).

Initially, di erent combinations of the electricity prices from 2019 and 2022, hydrogen prices of 1.3 and 5.5 €/kg$_{H_2}$, and electrolyzer capacities of 250, 500 and 750 MW were modelled. To establish a baseline of pro t, the traditional grid support case with all electricity injected into the grid was plotted in the same graphs. Across all electrolyzer capacities, the investment cost, amount of hydrogen produced and electricity supplied wasn't a ected by the hydrogen price. This is implied as there is no controller algorithm taking for example electricity prices into consideration. Figure 4.5 illustrates that the combination of the SE4 2019 electricity price and a 5.5 €/kg$_{H_2}$ hydrogen price was the only scenario where an electrolyzer investment gave higher pro ts than traditional grid injections. Using an electrolyzer investment cost of 1,576€/kW also resulted in a maximum pro t at a 500 MW electrolyzer capacity. In Figure 4.6 however, an electrolyzer investment was unpro table as the hydrogen price couldn't compete with the high electricity prices of 2022 in SE4. Figure 4.7 displays the relation between investment cost, hydrogen market price and electrolyzer capacity.

Given the SE4 2022 prices and a 50MW electrolyzer at 963€/kW, the hydrogen market price would have to increase to more than 9.2€/kg$_{H_2}$ in order to attain a pro table investment. Figure 4.7 illustrates this pro tability for two hydrogen prices and two investment costs. It is shown that an investment of 963€/kW requires a hydrogen price of 9.5€/kg$_{H_2}$, while this price was unpro table for the expensive investment. Hence, the gure displays how the pro t is a ected by a higher investment cost, showing that a higher electrolyzer investment cost would need an even higher hydrogen market price to compete with the electricity prices. For 1,576€/kW the hydrogen price had to be increased further, to 10€/kg$_{H_2}$.

Figure 4.7: Pro t from hydrogen production over the total system lifetime, as a function of electrolyzer capacity, for di erent market prices and investment costs. Compared to a traditional grid support case, see Table 4.1, which constitutes a pro t baseline by which the other cases can be compared. (Transfer capacity: unlimited. Electricity price: SE4 2022. Hydrogen market price: 8.5 vs. 9 €/kg$_{H_2}$).

It is expected that using a transfer limitation will increase the pro tability of hydrogen production as electricity incomes will be reduced, making hydrogen sales more competitive. Iterating the same con gurations for the other transfer capacities is left for future studies to evaluate.

4.3.1 Batteries

A grid transfer capacity of 500MW$_{peak}$ was used when evaluating the relevance of batteries in the hydrogen case since batteries were shown in Section 4.2.3.1 to be irrelevant for an unlimited capacity. Algorithm 5 was utilized to enable the batteries to operate properly, due to limitations in the software. This can be validated by the gures in Appendix D.2, where the batteries are seen to discharge their energy (upper graph in yellow) in order to prolong the electrolyzer operation (upper graph in green). A battery with high enough capacity would theoretically be able to maintain a constant electrolyzer production throughout the year, as shown by Figure D.6. It is seen that using a 3,730 MWh battery can keep the electrolyzer running at maximum capacity during most of the de cits displayed.

Table 4.7: Hydrogen case: battery addition con guration.

Parameter	Value
Controllers	
Positive electrical balance	Algorithm 5.
Negative electrical balance	1Battery.
	2. Grid extraction
Power grid	
Electricity price	SE4 2022
Grid transfer	500MW$_{peak}$

The pro tability of battery addition in the hydrogen case was seen to be decided by the electricity and hydrogen prices used in the system. The additional hydrogen income would need to exceed the sum of the battery investment and O&M, and also the previous electricity income that instead is used to charge the batteries. For the scenario of the SE4 2022 and 5.5 €/kg$_{H_2}$, adding 100 batteries results in an additional 60 tons of hydrogen produced, and 3.5 GWh less electricity injected into the grid, over the 20-year operational lifetime of the system. In total, this battery addition resulted in 4.8 M€ higher hydrogen sales and 7.5 M€ lower electricity sales, with a battery investment cost of 4.4 M€. Thus, the battery investment decreased pro ts to a large extent. This trend was seen even if the number of batteries was increased or reduced, con rming that batteries wouldn't result in higher pro ts. The model gave similar results with SE4 2019 electricity prices. The pro t decreased by 222 k€/MWh with 2022 electricity prices and 95 k€/MWh for 2019 prices.

Unlike the grid support case, where batteries were used to absorb unused peaks and discharge that energy during de cits, the hydrogen case with an added base load in the form of an electrolyzer had less peak energy to utilize in a battery. The technical lack of necessity for batteries, perhaps along with overestimated investment and O&M costs, are thought to be the main reasons why batteries couldn't produce more pro ts in a hydrogen-producing case. It was however seen that the additional investment resulted in a higher wind power utilization. As the case objective was to utilize batteries for the purpose of producing more hydrogen, hence the technical feasibility of battery addition can be con rmed.

4.4 Ammonia and methanol case

The e ect of di erent transfer capacities has been shown for the hydrogen case in Section 4.2.2 and is assumed similar for the NH$_3$ and MeOH cases. The main technical di erence is the continuous power consumption of the e-fuel production in question, which creates an additional power demand in the system. The new possibility to sell a more complex e-fuel was expected to shift the trade-o point between selling electricity or an e-fuel, towards e-fuels being more pro table. This was found to be especially dependent on the market price of the e-fuel. The di erences in both technical and economic characteristics of the two options are displayed in Table 4.8.

Table 4.8: Comparison of technical and economic characteristics of NH_3 and MeOH production.

Parameter	Ammonia	Methanol
	Synthesis	
Power cons.	1000 kWh/ton$_{NH3}$	720 kWh/ton$_{MeOH}$
Reactant power cons.	370 kWh/ton$_{N2}$	290 kWh/ton$_{CO2}$
Min. prod. rate	30%	40%
Synthesis ramping	1%/min	1%/min
Synthesis standby	Not allowed	Allowed
	Economics	
Investment cost	8,775¿/(kg$_{NH3}$/h)	7,100 ¿/(kg$_{MeOH}$/h)
Replacement	10 years á 30%	5 years á 20%
Annual O&M cost	1.5 %	4 %
Market price	450-1,500¿/ton$_{NH3}$	400-800¿/ton$_{MeOH}$

Further, the system con guration used for these cases is summarized in Table 4.9. The SE4 2019 electricity price was used along with an unlimited transfer capacity to enable some comparisons between grid injections and e-fuel production, while not having a competitive electricity price making all other alternatives obsolete.

Table 4.9: Ammonia and methanol case con guration.

Parameter	Value
	Controllers
Positive electrical balance	1. Electrolyzer. 2. Grid injection.
Negative electrical balance	1. Grid extraction.
	Power grid
Electricity price	SE4 2019
Grid transfer	Unlimited / 500MW$_{peak}$

4.4.1 Operational dynamics

To avoid catalyst degradation and maintain an e cient e-fuel synthesis, the minimum production rates along with standby modes and ramping times were taken into consideration. The di erences between NH_3 and MeOH synthesis had a visible e ect on the system operations, as shown in Figure E.1 and E.2. The electrolyzer was limited by the wind farm production potential while the NH_3 or MeOH synthesis was kept continuously running in sync with the hydrogen storage SoC. There is however a noticeable di erence in operation due to the standby mode frequently utilized by the methanol production unit. The fact that the NH_3 synthesis couldn't be put in standby, meant that a system with an insu cient H_2 storage wouldn't be able to run in Odyssey. The software instead returns an error message for a negative balance on the H_2 bus. Hence, hydrogen storage was a vital part of the NH_3 system.

The MeOH case however didn't experience the same in exibility. Far fewer H_2 containers were needed as allowing standby mode didn't cause the system to undergo any critical de cits a ecting the MeOH production. The MeOH case was able to operate even with no storage as a result of the standby mode, which could turn o the process if there wasn't enough hydrogen either produced or stored. Examining how the NH_3 system operates over a year, it could be seen that the H_2 storage was signi cantly over-dimensioned to handle a speci c occasion, approximately around the 1st of August, in order to avoid the balance error. Neglecting such occasions and optimizing the storage capacity according to what capacity is most frequently utilized would be more economically rational, as generally seen in the MeOH case.

4.4.2 Optimization process

This section will describe the process of optimizing the electrolyzer and hydrogen storage capacities, together with the NH_3 or MeOH production rate, as these parameters were seen to have a signi cant impact on the total pro t. Their individual in uences were also evaluated.

4.4.2.1 Ammonia production

The optimization process was extensive in the NH_3 case, as the production rate was a ected by the number of H_2 containers, as shown in Equation 3.1, and made it di cult to nd the global maximum for a static electrolyzer capacity. In the NH_3 case, the pro t could be maximized by reducing the hydrogen storage for each individual combination of di erent H_2 and NH_3 production rates. The storage capacity that was never utilized, i.e. the capacity from 0% up to the lowest SoC seen over a year, was an unnecessary overinvestment as this additional storage didn't provide either exibility or additional pro t.
For example, it was seen for the scenario of a 250 MW electrolyzer and a production rate of 26,000 kg_{NH_3}/h that 46 hydrogen containers gave the highest pro t. In contrast, 45 containers resulted in system failure due to a negative balance on the H_2 bus. Thus, 45 containers didn't provide su cient storage. If the number of containers instead was increased, the pro t decreased in relation to an increasing investment cost. The decrease in pro t from 46 to 200 hydrogen containers was 116 M¿, and the additional investment was 88 M€. When comparing this behavior to other cases, a similar trend is seen in the H_2 case (see Figure 4.4), con rming the energy system's typical reaction to a signi cantly increased storage capacity. Interestingly, the amount of NH_3 produced also decreased, while the amount of electricity supplied to the grid increased, as shown in Figure 4.8. This relation was unexpected, as it was thought that an NH_3 production depending on the H_2 SoC would be able to produce larger volumes when the storage capacity is increased. Resulting graphs from the system with 46 vs. 300 containers are displayed in Appendix E.1, and depict how the system using 300 containers (Figure E.4) never has to put the NH_3 production on standby due to a shortage of H_2 feedstock. The con guration with 46 containers (Figure E.3) has to put the NH_3 production on standby on several occasions, where the H_2 storage SoC (upper graph in blue) is seen to fall below the NH_3 production rate (upper graph in red). Comparing the two gures,

it can also be seen how the 46-container con guration is emptied faster than the 300-container. Keeping Equation 3.1 in mind, a frequently lower hydrogen storage SoC should be re ected in the total amount of NH_3 produced, implying that this behavior is unreasonable. Within the time frame of this study, an explanation for this was not possible to identify. A reasonable guess would be that Odyssey has an in-built self-discharge parameter, i.e. leakage, for each new H_2 container. It could however also be an unforeseen e ect of the H_2 storage SoC dependency, illustrated by Equation 3.2.

Figure 4.8: NH_3 production and electricity supplied vs. the number of hydrogen containers, with a 26 $tons_{NH_3}$/h production rate and 250 MW electrolyzer. (Transfer capacity: unlimited. Electricity price: SE4 2019.).

When the hydrogen storage has been minimized for various NH_3 production rates, all rates can be compiled to determine which production capacity would give the highest pro t. This is illustrated in Figure 4.9 using a 500 MW electrolyzer and a market price of 1,000¿/ton_{NH_3}. The gure distinctly presents how the production rate had a signi cant impact on the pro t, and that a maximum could be found. For this scenario, a production rate of 48 $tons_{NH_3}$/h gave the highest pro t.

Figure 4.9: Pro t from NH_3 production over the total system lifetime, as a function of the NH_3 production rate and at a constant hydrogen storage and electrolyzer capacity. (Transfer capacity: unlimited. Electricity price: SE4 2019. Market price: 1,000¿/ton_{NH_3}).

This process was then repeated for several electrolyzer capacities, resulting in a set of con gurations with optimized NH_3 production rates and H_2 storage capacities as shown in 4.10. Note that all con gurations have been optimized to maximize the pro t when a price of 1,000¿/ton $_{NH_3}$ is used. To further explain, it was seen that, when trying to maximize the pro t given a 450¿/ton $_{NH_3}$ price, the maximum was to not invest in an electrolyzer and ammonia process at all. Hence, the 1,000 price was used to attain the optimized relation between electrolyzer capacity, NH_3 production rate, and hydrogen storage.

Table 4.10: Optimized number of hydrogen storages for di erent combinations of electrolyzer capacities and NH_3 production rates (NH_3 market price: 1,000 ¿/ton $_{NH_3}$. Electricity price: SE4 2019. Transfer capacity: Unlimited).

Electrolyzer cap. [MW]	100	250	400	500	750	1,000
NH_3 prod. rate [tons$_{NH_3}$/h]	10	26	40	48	58	60
No. of containers	11	46	132	190	292	318
Max. mass stored [tons$_{H_2}$]	14	58	166	293	367	399

4.4.2.2 Methanol production

When optimizing the NH_3 case, the storage could be minimized until the simulation reached an error, meaning that the system was infeasible due to insu cient storage. Allowing standby resulted in a di erent optimization process in the MeOH case. However, the same three parameters (electrolyzer capacity, hydrogen storage capacity and MeOH production rate) were still found to have the largest impact on the system.
Initially, it was seen that by setting constant capacities for the H_2 storage and the electrolyzer, a maximized pro t could be found by increasing the MeOH price, as illustrated in Figure 4.10.

Figure 4.10: Pro t from MeOH production over the total system lifetime, as a function of the MeOH production rate, with a 500 MW electrolyzer and 15 hydrogen containers. (Transfer capacity: unlimited. Electricity price: SE4 2019. Market price: 400, 600, 800 and 1,500¿/ton $_{MeOH}$).

From the figure, it can be noted that a lower MeOH price of 400 or 600 €/ton $_{MeOH}$ didn't allow for the system to be optimized. This was because electricity injections were shown to result in larger profits than producing MeOH instead. For the 800 and 1,500 €/ton $_{MeOH}$ prices, a production rate of 50 tons $_{MeOH}$ /h gave the highest profits. It should also be noted how the profits initially decreased going from 0 to 10 tons $_{MeOH}$ /h using the ordinary price range of 400-800 €/ton $_{MeOH}$ prices, after which the profit was increased for the 800 €/ton $_{MeOH}$ price.

Switching the varying parameter from the MeOH production rate to the number of hydrogen containers, gave some more insight into how the system could be optimized. Figure 4.10 illustrate the relation between profit and hydrogen storage capacity, for a 100 MW electrolyzer and a 10 tons $_{MeOH}$ /h production rate. It is seen that, for a market price of 1,500 €/ton $_{MeOH}$, the profits and amount of produced MeOH are increased when increasing the storage to 2 containers, after which an increased storage capacity results in a slowly decreasing profit. The electricity supplied to the grid is also shown to decrease when increasing the number of containers.

Figure 4.11: Profit from MeOH production over the total system lifetime, as a function of the number of hydrogen containers, with a 100 MW electrolyzer and a rate of 10,000 kg $_{MeOH}$ /h. (Transfer capacity: unlimited. Electricity price: SE4 2019. Market price: 600 and 1,500 €/ton $_{MeOH}$).

Figure 4.12 illustrates the same behavior but for a 400 MW electrolyzer and a 39 tons $_{MeOH}$ /h production rate. By comparing these two figures, an understanding can be established of how the significant change in profit is relocated depending on the electrolyzer capacity and MeOH production rate. This was a result of the minimum H_2 consumption connected to the MeOH production, as an increased production rate increased the lowest required amount of H_2 available.

Figure 4.12: Pro t from MeOH production over the total system lifetime, as a function of the number of hydrogen containers, with a 400 MW electrolyzer and a rate of 39,000 kg_{MeOH}/h. (Transfer capacity: unlimited. Electricity price: SE4 2019. Market price: 600 and 1,500 €/ton_{MeOH}).

Figure 4.12 also displays how a maximized pro t (though still negative) can be found for a high enough MeOH price, while the 600 €/ton_{MeOH} price still experiences that signi cant pro t increase going from 5 to 6 containers. However, for this scenario, an initial pro t increase was seen when increasing from 3 to 4 containers, as this was found to be a signi cant breaking point of how often the MeOH unit had to be put on standby. This relation is further illustrated in Figure 4.13.

Figure 4.13: MeOH production and electricity supplied vs. the number of hydrogen containers, with a 39 $tons_{NH_3}$/h production rate and 400 MW electrolyzer. (Transfer capacity: unlimited. Electricity price: SE4 2019.).

Note how this relation is inversely proportional to what was seen in the NH_3-case, see Figure 4.8, i.e. that an increased number of H_2-containers will increase the amount of MeOH produced, but decrease the amount of NH_3. This behavior was very much expected, as the production rate correlates to the H_2-storage SoC according to Equation 3.1.

One conclusion that can be drawn by comparing Figure 4.11 and 4.12, is that the amount of MeOH produced is directly connected to the H_2 storage capacity when the MeOH production rate and electrolyzer capacity is kept constant. By increasing the number of containers beyond what's shown in the figures, the profit would decrease linearly in relation to the H_2 storage investment cost. That could however be a relevant option if the main objective would be to maximize the MeOH production instead of the profit. This would however be very capital intensive.
In the end, the system was optimized by varying the MeOH production rate and the number of H_2 containers. For similar results as shown in Figure 4.12, the configurations with the highest profit in relation to the most amount of MeOH produced were used.

Table 4.11: Optimized numbers of hydrogen containers for different combinations of electrolyzer capacities and MeOH production rates (MeOH market price: 600 €/ton $_{MeOH}$. Electricity price: SE4 2019. Transfer capacity: Unlimited).

Electrolyzer cap. [MW]	100	250	400	550	750
MeOH prod. rate [tons$_{MeOH}$/h]	10	24	39	53	69
No. of containers	2	7	8	13	12
Max. mass stored [tons$_{H_2}$]	2.5	8.8	10	16	15

4.4.3 Economic performance

Table 4.10 and 4.11 show the optimized configurations of the NH_3 and MeOH cases. One interesting observation from these tables is that, unlike the NH_3 case, the hydrogen storage decreased when increasing the electrolyzer capacity from 550 to 750 MW in the MeOH case. The reason for this could be that the electrolyzer was large enough to decrease the required amount of storage while still maintaining a high MeOH production rate. Regardless, the economic performance of the summarized configurations was evaluated primarily by comparing the resulting profit for different e-fuel market prices. The results are compiled in Figure 4.14 and 4.15, and clearly points towards NH_3 being the most attractive option.

Figure 4.14: Profit from NH_3 production over the total system lifetime, as a function of electrolyzer capacity, for different market prices. Compared to a traditional grid support case, see Table 4.1, which constitutes a profit baseline by which the other cases can be compared. (Transfer capacity: unlimited. Electricity price: SE4 2019. Market price: 450, 1,000 and 1,500 €/ton $_{NH_3}$).

Figure 4.15: Pro t from MeOH production over the total system lifetime, as a function of electrolyzer capacity, for di erent market prices. Compared to a traditional grid support case, see Table 4.1, which constitutes a pro t baseline by which the other cases can be compared. (Transfer capacity: unlimited. Electricity price: SE4 2019. Market price: 400, 600 and 800 €/ton $_{MeOH}$).

It can be seen that only one market price could make the MeOH case more pro table than traditional grid injections, while the NH_3 case appeared more promising. Using a price of 800 €/ton $_{MeOH}$, a maximized con guration should be attained in the 100-250 MW electrolyser capacity range. In the NH_3 case, an electrolyzer capacity of around 300-500 MW gave the highest pro t using a 1,000 €/ton $_{NH_3}$ price, while increasing the price to 1,500 resulted in an electrolyzer of 500-800 being the most pro table. Further, it was found that a MeOH market price of 2,000 €/ton $_{MeOH}$ was needed to make MeOH production as pro table as a scenario with a 1,500 €/ton $_{NH_3}$ price.

4.4.3.1 500 MW transfer capacity

Evaluations of the operational dynamics and optimization process were made under the assumption that a future e-fuel-producing setting will allow for all the excess electricity to be injected into the grid. This will however not always be the case. Assuming that the operational dynamics will remain, una ected by the transfer capacity, the system con gurations shown in Table 4.10 and 4.11 will still be the most optimal ones from a technical aspect. The same con gurations were used to produce Figure 4.16 and 4.17, in order to illustrate the e ect of the transfer capacity on the nal pro t when producing NH_3 and MeOH.